The RNA splicing factor Prp45 plays an evolutionarily conserved role in histone H2B ubiquitination

Amit Paul, Ph.D.[1, 2] and Tracy L. Johnson, PhD [1, 2, 3]

[1]Department of Molecular Cell and Developmental Biology, University of California, Los Angeles, CA, USA, 90095

[2]Molecular Biology Institute, University of California, Los Angeles, CA, USA, 90095

[3]To whom correspondences should be addressed:

Tracy L. Johnson, UCLA Department of Molecular Cell and Developmental Biology,
610 Charles E Young Dr. S, Los Angeles, CA 90095
Tel (310) 206-2416; E-mail: tljohnson@ucla.edu

Abstract

The yeast protein Prp45 (mammalian SKIP) has a well-characterized role in RNA splicing. While Prp45/SKIP has been implicated in transcription elongation in metazoans, the mechanism for a role for the yeast protein outside of splicing is unclear. The C-terminus of Prp45/SKIP is intrinsically disordered and contains a highly conserved helical domain, although the function of these regions has remained enigmatic. Here, we show that the C-terminus of Prp45 plays a previously unknown role in histone H2B ubiquitination, a mark of active elongation. Genetic, proteomic, and biochemical analyses reveal that the C-terminal region of the protein functionally and physically interacts with proteins involved in histone H2B ubiquitination. Prp45 associates with Lge1, the scaffold protein that is essential for the activity of the H2B ubiquitin ligase complex, and this interaction is necessary to stabilize Lge1 for interaction with the Bre1 ubiquitin ligase. In the absence of the Prp45 C-terminus interactions, cells show a severe loss of H2B ubiquitination and the “Large” (Lge1) phenotype associated with H2B ubiquitination defects. Lge1 stability, H2B ubiquitination, and proper cell morphology are all restored by reintroduction of the C-terminal IDR/helical domain from not only *S. cerevisiae*, but also from plants or humans. These results demonstrate an extra-spliceosomal role for the C-terminus of Prp45/SKIP in chromatin modification and proper cellular function.

Keywords: Prp45, Intrinsically Disordered, chromatin modification, H2B ubiquitination, Lge1, Bre1, transcription elongation, *Saccharomyces cerevisiae*

Introduction:

Since the discovery of introns in eukaryotic genes, elegant studies of the multi-subunit complex that recognizes these noncoding sequences have revealed that the spliceosome assembles onto a pre-messenger RNA in a stepwise manner, co-transcriptionally, while the RNA is being synthesized by RNA polymerase II through a chromatin template. A critical step in spliceosome assembly is the formation of the activated complex when the Prp19 complex (NTC) and NTC-associated factors (Prp45, Prp46, etc.) bind to the tri-snRNP complex.[1,2,3] The NTC plays a crucial role in mediating spliceosome rearrangements necessary for catalysis.[2,4] Both sequence predictions and the high-resolution Cryo-EM structure of the isolated activated complex reveal that one of the NTC-associated factors, Prp45, contains an intrinsically-disordered C-terminal region that appears to extend out of the complex,[5,6] perhaps serving as a site for interaction with other splicing factors during stepwise assembly or other proteins in the proximity of the spliceosome.

Prp45 is essential for cell viability. Nonetheless, the cell can tolerate extensive truncation of Prp45 at its C-terminal end. Prp45, containing only the first 169 out of the total 379 amino acids, grows normally at 30°C, but growth is significantly impaired when the temperature is raised to 37°C.Prp45 deleted of this C-terminal region (Prp45ΔCTR) shows reduced interaction with the second step helicase Prp22, thus affecting the fidelity of 3' splice site selection and the splicing of those genes that lack the optimal distance between the branchpoint and 3' splice site or that contain non-consensus 3' splice sites. Moreover, Prp45 lacking this C-terminal region exhibits defects in splicing a subset of genes.

We previously showed that co-transcriptional assembly of the spliceosome at the step of Prp45 association is influenced by transcription elongation and the state of the chromatin. During transcription elongation, the Set2 histone methyl transferase methylates histone H3 at lysine 36 (H3K36me), a mark of active transcription.[10-12] H3K36 methylation is recognized by the chromodomain-containing protein Eaf3[13,14,15] which, in turn, stabilizes the co-transcriptional association of Prp45 and the recruitment of the Prp19 complex.

These interactions facilitate co-transcriptional splicing.[14] As this example illustrates, there is strong evidence that histone modification affects RNA splicing, a relationship that is intuitive given the spatial and temporal proximity of the two reactions. The inverse relationship, that splicing factors affect chromatin modification, has also been described, particularly in metazoan cells.[16,17] However, direct mechanisms by which splicing factors affect chromatin modification have been difficult to determine. Prp45 is an intriguing candidate for such a role, given its activity at the interface of the two reactions.

The homolog of Prp45, SKIP (Ski-interacting protein), in *Arabidopsis thaliana* and *Homo sapiens* has been shown to play a role in transcription.[18,19] SKIP interacts with the Paf1 complex and activates FLC transcription to control flowering in Arabidopsis.[19,20] In humans, SKIP associates with the Positive Transcription Elongation Factor b (pTEFb) to facilitate transcription elongation by HIV-1 Tat.[18] While a role in transcription has not been clearly demonstrated in yeast, the yeast protein Prp45, when fused to the DNA-binding domain of SKIP, can activate transcription.[7] Intriguingly, Prp45 shows genetic interactions with several chromatin-related enzymes, including strong interactions with Htz1 and the Swr1 complex members.[21]

H2B monoubiquitination is an important mark that modulates the global chromatin landscape and acts upstream of other key histone modifications associated with transcription elongation, such as H3K4 methylation[22,23] and H3K36 methylation.[24,25] Bre1 is an E3 ligase that mono-ubiquitinates histone H2B at lysine 123 in the coding region during pol II elongation, in collaboration with the E2 conjugating enzyme Rad6.[22,26] A third protein, Lge1, which was originally identified in a screen for gene deletions that lead to a Large (LarGE) cell phenotype,[27] is essential for Bre1 catalytic activity. Although Lge1 is largely unstructured, the coiled-coil (CC) domain of Lge1 interacts with the N-terminal region of Bre1, and this interaction is necessary for Bre1-mediated H2BK123 ubiquitination in yeast.[28] Proper distribution of histone H2B monoubiquitination is necessary for gene activation and is regulated by cycles of deubiquitination. The de-ubiquitinase Ubp8, which is part of the SAGA complex, deubiquitinates H2B, particularly at the 5' end of genes.[24]

Here, we combine genetics, proteomics, and biochemical approaches to show that the C-terminal region of the Prp45 protein both physically and functionally interacts with proteins involved in histone H2B ubiquitination. Consistent with these interactions, we find that the C-terminal region of Prp45 is required for efficient histone H2B monoubiquitination. To understand how Prp45 affects H2B monoubiquitination, we analyzed its interactions with the ubiquitin ligase complex and found that Prp45 physically interacts with Lge1 and that truncation of Prp45 destabilizes Lge1. While Lge1 forms discreet puncta in WT cells, as Lge1 is destabilized, its ability to form puncta is significantly reduced, and its binding partner, Bre1, escapes the nucleus. Consistent with a role for the C-terminal portion of Prp45 in Lge1 stability, truncation of Prp45 shows the "large" cell morphology similar to *lge1*Δ, which can be reversed by deletion of the de-ubiquitinase, indicating that the C-terminal domain of Prp45 has global effects on cellular morphology via a mechanism that involves H2B monoubiquitination.

The C-terminal region of Prp45 bears a striking similarity to the C-terminus of SKIP, including approximately 50 amino acid regions with propensity to form helical structure. Here, we show that the C-terminal homologs of Prp45 from higher eukaryotes (*At* SKIP & *Hs* SKIP) can replace the yeast C-terminus and recapitulate the chromatin modification and cell morphology phenotypes, suggesting both sequence and functional conservation of the C-terminal region of Prp45/SKIP.

Results

The C-terminal portion of Prp45 is required for optimal cell viability

Previous studies provided evidence that Prp45 is recruited co-transcriptionally and in close proximity to the chromatin.[14] Prp45 contains an SNW domain (amino acids 1-169) that is essential for viability. The C-terminal region encompasses a helical domain and the SH2-like domain, which, in isolation, is predicted to be highly disordered, as illustrated by analysis using AIUPred [29] (Figure 1A).

The homologs of Prp45 in Arabidopsis (*At* SKIP) and Humans (*Hs* SKIP) are also spliceosome components. Although the amino acid sequence of the C-terminus is different from yeast (Figure S1), they share a striking structural similarity (Figure 1B). Interestingly, the conserved alpha-helical domain, thought to be a site of protein-protein interactions, is approximately 52 amino acids long across species (Figure 1B).

To begin to evaluate the function of this disordered, C-terminal region of the protein, we generated truncation mutants of Prp45; *prp45 (1-169)*, *(1-174)*, *(1-184)*, *(1-260)* and *(1-296)*, where the residues after 169, 174, 184, 260, and 296 were deleted, and the cells were grown at 30°C and 37°C (Figure 1C). The largest truncation, which eliminates the helical domain and a linker region between the SNW and the helical domain, *prp45 (1-169)* or *prp45ΔCTR*, shows the most dramatic growth defect at elevated temperature. The strains with the second-largest growth defects, *prp45 (1-174)* and *prp45 (1-184)*, eliminate the helical domain while retaining the linker region. *prp45 (1-260)* and *prp45 (1-296)*, containing the region beyond the predicted disordered regions, grow similarly to wild-type cells at 37°C (Figure 1C). These results suggest that the disordered region of Prp45 that has a propensity to form helical structure is important for its function, warranting a more detailed exploration of the domain's protein-binding properties and potential interactors.

The Prp45 C-terminus interacts with the H2B ubiquitination machinery and is critical for H2B ubiquitination

To identify specific proteins that interact with Prp45 via the C-terminal region, proximity labeling was performed. Briefly, biotin ligase BirA was added to the C-terminal region of either full-length Prp45 or Prp45ΔCTR, and the strains were grown in the presence of biotin. The biotinylated proteins were immunoprecipitated using streptavidin beads, followed by mass spectrometry (Figure S2A). Full-length Prp45 interacts with 251 different proteins. Of these, 213 proteins show differential interactions when the C-terminal end is truncated (Figure S2B). We first focused on those with a significant decrease in interactions, then on those in which interactions were lost upon truncation of the C-terminal end. Not surprisingly, most of the abrogated interactions are with known splicing factors, such as Prp19, a fellow member of the NTC. The interactions between Prp45 and Brr2, Clf1, Prp46, and Spp2 are significantly reduced in Prp45ΔCTR, compared to the wild type (Figure S2C).

Thirty-eight proteins are not detected at all when the C-terminus is truncated, suggesting that their interactions with Prp45 are dependent on the C-terminus (Table S1). Hierarchical clustering of the 38 proteins reveals that the largest class of proteins is involved in RNA splicing. Nevertheless, an intriguing subset is implicated in transcription elongation and chromatin function (Table S1). One of the interactions lost when the C-terminus of Prp45 is deleted is with Bre1, the E3 ligase that, together with its E2, Rad6, monoubiquitinates histone H2B.[30,31] Monoubiquitination of H2B requires a third component of this complex, Lge1, which interacts directly with Bre1 and is required for Bre1's H2B-ub activity.[32,33]

To determine if there is a functional relationship between H2B monoubiquitination and the Prp45 C-terminus, *BRE1*, *RAD6*, and *LGE1* were each deleted in combination with *prp45ΔCTR,* and the strains were grown at 30°C (data not shown) and 37°C. While growth of the double mutants is not significantly impaired at 30°C, at 37°C, *prp45ΔCTR bre1Δ*,

prp45ΔCTR rad6Δ, and *prp45ΔCTR lge1Δ* all show a growth defect compared to *prp45ΔCTR*; *prp45ΔCTR bre1Δ* and *prp45ΔCTR lge1Δ* are barely inviable (Figure 2A).

Since mutations that abrogate H2B monoubiquitination show strong negative genetic interactions with Prp45, we predicted that mutations that stabilize monoubiquitination would reverse the *prp45ΔCTR* growth defect. Ubp8 and Sgf73 are members of the SAGA complex and contribute to histone H2B deubiquitination.[34-37] Deletion of either *UBP8* or *SGF73* in the *prp45ΔCTR* strain partially rescues the growth defect at 37°C (Figure 2A, right image), with deletion of *UBP8*, the gene encoding the catalytic protein, showing the strongest suppression.

Considering the functional and physical interactions between H2B ubiquitination machinery and Prp45, H2B ubiquitination was assessed in cells harboring a Prp45 C-terminal truncation. Analysis of the ubiquitinome (Figure 2B schematic) from wild-type and *prp45ΔCTR* cells reveals a significant reduction in peak intensity of H2BK123 peptides in *prp45ΔCTR* (Figure 2B). Immunoblot analysis shows a significant reduction in H2BK123 ubiquitination in *prp45ΔCTR* at 37°C. In fact, there is an approximately 90% decrease in H2BK123ub in the *prp45ΔCTR* strain, although the levels of H2B remain the same (Figure 2C). Hence, the C-terminal domain of Prp45 affects H2BK123 ubiquitination, likely by modulating the catalytic activity of Bre1, the ubiquitin ligase.

Since deletion of *UBP8* partially rescues the growth defect in *prp45ΔCTR,* it seemed likely that it would also rescue the H2BK123 ubiquitination defect. Indeed, restoration of H2BK123 ubiquitination is observed in *prp45ΔCTR ubp8Δ* (Figure 2D), consistent with the observation of a partial rescue of the *prp45ΔCTR* growth defect when *UBP8* is deleted. Notably, although H2B ubiquitination is restored, growth is partially restored, which points to a contribution of the other functions of the C-terminal domain in addition to its role in H2B ubiquitination for optimal growth.

While disordered proteins are susceptible to proteasomal degradation,[38 39] recent studies of intrinsically disordered regions of proteins show that IDRs by themselves decrease the

thermodynamic stability of proteins but can increase the intrinsic structural stability of multidomain proteins or protein complexes that exhibit complex conformational dynamics.[40-42] Hence, we considered the possibility that Prp45ΔCTR is less stable than the full-length Prp45 protein at 37°C. Indeed, the results show this to be the case (Figure S3A left). No significant difference in RNA expression is observed (Figure S3A right). This suggests that the C-terminal domain is required to maintain the stability of the Prp45 protein, particularly at elevated temperatures. To further support this hypothesis, full-length Prp45 and Prp45ΔCTR were each degron tagged and grown on YPD + IAA plates at 30°C and 37°C. Growth of the Prp45 degron strain is significantly reduced compared to the wild-type cells, and the Prp45ΔCTR degron strain grows even more slowly (Figure S3B left image). At 37°C, the Prp45ΔCTR degron strain does not grow at all (Figure S3B right image). Interestingly, at 37°C, the Prp45 degron strain maintains robust growth, suggesting that an altered structure in the C-terminal domain limits its degradation, even in the presence of auxin (Figure S3B, right). While deletion of *UBP8* can suppress the defect in H2B ubiquitination when Prp45 is truncated, it does not, not surprisingly, increase the protein's stability (Figure S3C). Deletion of *UBP8* in the *prp45ΔCTR* degron strain does not rescue the growth defect on the IAA plate (Figure S3D), further supporting a unique role of the C-terminal domain in maintaining protein stability. These data suggest that at higher temperatures, the C-terminal disordered domain of Prp45 adopts a conformation that increases its stability and enables interactions that promote H2B ubiquitination.

The C-terminal domain of Prp45 interacts with and stabilizes the ubiquitin ligase scaffold protein, Lge1

Although Bre1 is the ubiquitin ligase responsible for H2B monoubiquitination, Bre1's activity is dependent on the Lge1 protein, especially when the cells experience replicative stress.[43] A recent analysis of the Lge1-Bre1 interaction reveals that Lge1 phase separates and forms condensates, which is mediated by its intrinsically disordered domain. The coiled-coil (CC) domain of Lge1 interacts with the middle, or Lge1 binding domain (LBD), of Bre1, and this interaction is necessary for Bre1-mediated H2BK123 ubiquitination.[28]

Although Lge1-deleted cells can normally grow at 30°C and 37°C, they are morphologically larger than wild-type cells. A recent study of the mammalian proteins responsible for H2B ubiquitination shows that RNF20/RNF40, the mammalian homolog of Bre1, interacts with the conserved coiled-coil domain of WAC protein (WAC-CT) (Lge1 homolog in mammals), and this interaction is crucial for H2B ubiquitination.[44]

While proximity labeling provides insights into the physical distance between two proteins, it is difficult to assess whether these interactions are direct or indirect since any protein residing within a 10 nm diameter can be biotinylated.[45] In light of the observation of a Prp45 C-terminus-dependent interaction with Bre1, we sought to detect interactions between these proteins by co-immunoprecipitation but could not detect a physical interaction between Bre1 and Prp45 (data not shown), suggesting that the interaction observed by proximity labeling may be weak and/or indirect. We therefore considered proteins that are part of the H2B ubiquitination complex to determine whether they interact with Prp45, starting with Lge1, the Bre1 cofactor required for its catalytic activity.[33] Full-length Prp45 immunoprecipitates Lge1, and the interaction is reduced when the C-terminus of Prp45 is truncated (Figure 3A). Based on the known structural information for Prp45 and Lge1, AlphaFold-multimer in Google Colab Fold[46] was used to predict protein-protein interacting regions between the proteins. The *in-silico* analysis suggests interactions at the C-terminal region of Prp45 and a structured coiled-coil (CC) domain of the Lge1 protein (Figure S4A left image)

Although Lge1 is a highly disordered protein, with most of its residues (~85%) residing in disordered regions, as illustrated in Figure S4A (right image), it also contains a short, structured coiled-coil (CC) domain through which it interacts with other proteins, such as Bre1.[28] Not surprisingly, deletion of the CC domain leads to loss of H2B monoubiquitination, comparable to that observed with a *BRE1* deletion (Figure S4B). When the CC domain of Lge1 is deleted in the *prp45ΔCTR* strain, and cells are grown at 37°C, these cells are nonviable, and the phenotype is comparable to the *prp45ΔCTR lge1Δ* strain or *prp45ΔCTR bre1Δ* (Figure S4C, Figure 2A). Interestingly, deletion of the CC domain also causes the cell to become large, as in the Lge1-deleted cell (Figure S4D).

These data suggest that Prp45's effects on the catalytic activity of Bre1 are likely through its interactions with Lge1. While we cannot rule out the possibility that Prp45 interacts directly with *both* Lge1 and Bre1 (perhaps weakly in the case of the latter), Prp45 interacts with Lge1, and the Lge1-Bre1 activity is dramatically affected by the Prp45 C-terminus.

In light of reports that Lge1 is a disordered protein and that interactions with proteins at its CC domain (e.g., Bre1) determine its stability,[33] we considered the possibility that Lge1's interaction with the C-terminus of Prp45 is an important contributor to its stability. To determine if this is the case, Immunoblot analysis of Lge1 protein was performed in wild-type and *prp45ΔCTR* strains. Although *LGE1* RNA levels remain unchanged (Figure 3B, right), the Lge1 protein becomes unstable in the *prp45ΔCTR* strain when compared to the Lge1 protein isolated from wild-type cells, particularly at 37°C (Figure 3B, left).

To further assess whether Prp45 contributes to Lge1 stability, Lge1 protein levels were analyzed in an auxin-inducible degron strain, where Prp45 was degraded in the presence of IAA over time (0, 15', 30', 60'). Indeed, Lge1 levels decrease in a time-dependent manner, with kinetics like Prp45 (Figure 3C). H2BK123 ubiquitination levels are also gradually reduced during the degradation of Prp45 and Lge1. When cells are exposed to DMSO at the same time points, Lge1 protein levels remain unchanged, indicating IAA (and hence Prp45) dependent loss of Lge1 (Figure 3C) abrogates H2B ubiquitination.

To look at the relationship between the Prp45 CTR and Lge1 stability another way, Lge1 CDS was tagged with a degron at its C-terminal end, and a Kanamycin resistance marker was included at the N-terminal end under the native Lge1 promoter. The rate of degradation of Lge1 protein was examined in the wild type or the *prp45ΔCTR* strain by assaying Kan^r (Figure 3D, schematic). When the cells were grown and serially diluted on a YPD + Kanamycin + IAA plate (Figure 3D), the results show a clear growth difference between the Lge1 degron in the wild-type background vs. the *prp45ΔCTR* strain on the Kanamycin plates. Degradation of Lge1 in the presence of IAA causes loss of kanamycin resistance; the *prp45ΔCTR* exacerbates the growth defect, consistent with enhanced Lge1 destabilization when the CTR of Prp45 is absent (Figure 3D).

Loss of Lge1 leads to a decrease in Lge1-dependent nuclear puncta and altered Bre1 distribution

Lge1 was first identified in a screen for genes whose deletion disrupted cell size homeostasis. Although *LGE1* is not essential for cell viability, morphologically, the cells appear to have this large phenotype when *LGE1* is deleted.[27] Lge1 forms puncta in the nucleus to locally concentrate Bre1.[28] Since Prp45 degradation leads to unstable Lge1 protein, we predicted that puncta formed by the Lge1 protein would also be reduced. To test this prediction, Lge1 was GFP-tagged in the Prp45 degron strain, and cells were grown in the presence of IAA or DMSO, followed by confocal microscopy. Indeed, GFP intensity is significantly reduced in the presence of IAA (Figure 4A) compared with the DMSO control. Lower GFP intensity was quantified and confirmed using cell pose[47] (Figure 4B right). The quantification also revealed that cells become larger when Prp45 is degraded (Figure 4B left), similar to the phenotype observed when H2B ubiquitination is reduced.[48] To determine how this decrease in Lge1 and Lge1-containing puncta affects Bre1 activity, Bre1 was GFP-tagged in wild-type and *prp45ΔCTR* cells. While Bre1 is highly concentrated in the nucleus in WT cells, it is evenly distributed between the nucleus and cytoplasm in prp45 CTR cells (Figure 4C). We further confirmed this observation using a protein transit assay in which the nuclear histone protein H2A.Z or the cytoplasmic protein Pgk1 was turboID (Biotin ligase or Bir A) tagged in cells with either WT Prp45 or Prp45 with a deleted C-terminal end. The cells were grown in the presence of biotin, and the biotinylated proteins were pulled down with streptavidin beads. Bre1 was detected using an anti-GFP antibody, as it was N-terminally GFP-tagged and expressed from the plasmid. If Bre1 protein is largely chromatin-bound, as we suspect is the case in wild-type cells, then more Bre1 will be biotinylated in the Htz1-turboID cells, and less will be biotinylated in the cytoplasmic Pgk1 TurboID cells (Figure 4D & graph). If the distribution is altered as in *prp45ΔCTR* cells, we expect to see more Bre1 biotinylated in the cytoplasm by PGK1 TurboID relative to the levels observed in WT cells, which is precisely what is observed (Figure 4D & graph).

Previous studies have shown that when the C-terminus of Prp45 is truncated, cells are also large, elongated, and highly heterogeneous.[9] As described above, in a comparison between the cell sizes of *prp45ΔCTR* and *lge1Δ*, relative to WT cells, *prp45ΔCTR* cells are almost 2.5 times larger than the wild type cells and similar in size to *lge1Δ* cells (Figure S4D). Moreover, since H2B ubiquitination has been shown to be involved in maintaining cell size,[48] it was satisfying to see that stabilizing H2B ubiquitination by deleting *UBP8* reverses the elongated-cell phenotype and restores cell size in *prp45ΔCTR* (Figure 4E).

As shown in Figure 1, the highly disordered domain of Prp45 extends to the conserved SH2 domain of the protein, and the region of the protein up to the SH2 domain that includes the disordered region is sufficient to confer near WT growth (Figure 1). To clarify that, indeed, the disordered portion of the C-terminus is sufficient to confer the H2B ubiquitination functions, a Prp45 truncation containing the disordered region of the C-terminus, *prp45 (1-260),* was analyzed to assess each of the phenotypes associated with *prp45ΔCTR*. Prp45 stability (Figure S5A), Lge1 stability (Figure S5B), H2B ubiquitination (Figure S5C), and cell size homeostasis (Figure S5D). As with growth, *prp45 (1-260)* is sufficient to restore near-WT activity.

Trans-expression of Prp45's C-terminal region in the *prp45ΔCTR* strain rescues the slow growth phenotype and H2B ubiquitination

The C-terminal portion of Prp45, containing the disordered domain, is critical for Prp45 function in chromatin modification. This region of Prp45 also contributes to its stability and to its ability to interact with and modulate the activity of the H2B ubiquitination machinery. Given these findings, we considered the possibility that the C-terminus could act in trans with the N-terminal part of the protein to affect Prp45 function. To test this, the C-terminal domain of Prp45 (170-379) was cloned into a yeast 2μ plasmid under the native Prp45 promoter and expressed in the *prp45ΔCTR* strain. Intriguingly, the C-terminus expressed in trans rescues the growth defect (Figure 5A). The C-terminus of Prp45 contains a 5-amino-acid-residue SNWKN motif, which is identical in all genera (Figure S1).[20] To

determine if this motif is required for the C-terminus to restore growth, the SNWKN motif was removed from the trans expressed protein. Despite its conservation, the SNWKN motif is required for the C-terminus to restore viability. (Figure 5A).

To determine if the C-terminus expressed in trans can rescue the chromatin-related phenotypes, Lge1 stability was assessed when the C-terminal domain (170-379) was expressed in the *prp45ΔCTR* strain. Trans expression of the C-terminal domain stabilizes the Lge1 protein in the *prp45ΔCTR* strain (Figure 5B-C). Moreover, the trans-expressed C-terminal domain in *Kan^r CDS-Lge1 degron prp45ΔCTR* strain partially restores growth on Kan + IAA plate in the presence of IAA, indicating that Lge1 becomes more stable and less susceptible to proteasome-mediated degradation in the presence of the C-terminus (Figure 5C). Since trans expression of the C-terminal domain stabilizes the Lge1 protein, we predicted that it would also rescue H2B ubiquitination. Indeed, not only is H2B ubiquitination restored (Figure 5D), but so are proper cell morphology and size (Figure 5E & graph).

The observation that the two halves of Prp45 can function on separate molecules suggests that the N- and C-termini of the protein may make functional interactions. Data from both Dictyostelium and *S. Pombe* Prp45 show strong evidence of Prp45 dimerization.[49] Furthermore, when Prp45 is analyzed using AlphaFold, not only is dimerization predicted, but the modeling also predicts interactions between the N- and C-termini of the proteins (data not shown). Additionally, Co-IP between the C-terminus and the N-terminus suggests that the halves of the proteins can interact, although the interaction appears to be weak and/or dynamic (Data Not Shown).

To determine if the C-terminus of Prp45 can function independently of the N-terminus, we expressed just the C-terminal portion of the protein alone to determine if it could suppress the lethal phenotypes associated with the Prp45 deletion. *prp45Δ* strains containing only the C-terminal domains (170-379, 175-379, 184-296) after the WT plasmid was “shuffled out” were analyzed for growth on 5-FOA. The C-terminus alone does not restore *prp45Δ* growth on SC-FOA plates (Figure S6A).

The C-terminus of Arabidopsis and Human SKIP restore activity of *prp45*Δ*CTR*

The fact that the C-terminal domain, expressed in trans, can partially restore growth and H2B ubiquitination highlights the importance of this disordered region. As shown in figure 1B, this feature of the protein is highly conserved, down to the size of the predicted region of helical propensity, suggesting that homologs of Prp45 may also stabilize interactions that drive H2B ubiquitination. To test this, the C-terminal domains from *Arabidopsis* (*At* C-SKIP) and Human fibroblast (*Hs* C-SKIP) were cloned into a yeast 2μ plasmid to determine if they could restore Prp45 functions in trans. The C-terminal domains from *At* and *Hs* alone could not rescue the growth defect (Figure 6A upper image). However, when At SKIP was fused to the N-terminus of the yeast protein, *Sc_At prp45 Chimera* [*Sc* Prp45 (1-169) + *At* (C-terminal domain], strong rescue of the growth defect was observed (Figure 6A middle image), suggesting that placing this domain in proximity of the N-terminus is critical for growth rescue.

Previous studies of Prp45 report that overexpression of either the *Arabidopsis* or human SKIP protein can replace the yeast protein.[20] However, when either of these proteins is expressed from the yeast 2μ plasmid in the absence of Prp45 (*prp45*Δ strain), little 37°C growth rescue is observed (Figure S6A). On the other hand, when either *At* or *Hs* SKIP in the yeast 2μ plasmid is expressed in *the prp45*Δ*CTR* strain, where the N-terminal portion of the protein is present, the full-length SKIP proteins can rescue the growth defect (Figure 6A, lower growth assay image), with the A*t* SKIP conferring better rescue. Together, these data suggest an evolutionarily conserved function for the C-terminus of Prp45/SKIP and support a model whereby protein interaction between the C- and N-termini (such as through dimerization of the proteins) is important for their functions.

The observation that the chimera protein can support growth suggests that these protein interactions also form a surface that supports Lge1 interaction and stability, Lge1 activity, and proper H2B ubiquitination. Lge1 stability was evaluated as described in Figure 3D, in which the stability of the protein was assessed by growth on the Kanamycin + IAA plate.

The cells grow well, indicating that Lge1 is stabilized by the chimeric protein (Figure 6B). Moreover, H2B ubiquitination is also restored when *At* SKIP is fused to Prp45ΔCTR (Figure 6C & 6F, lower panel). With the restoration of H2B ubiquitination, we predicted that aberrant cell morphology and size would also be restored by the chimera, as we observe (Figure 6D). We also assessed the stability of the chimera and found that the protein is indeed more stable than the Prp45ΔCTR protein (Figure S6G).

The C-terminal portion of the Human SKIP protein behaves similarly when fused to Prp45ΔCTR. A chimera protein comprised of the C-terminal half of Human SKIP and the N-terminus of *Sc* prp45 (*Sc_Hs* prp45 chimera) not only restores the growth (Figure S6C), but also H2B monoubiquitination, chimeric protein stability (Figure S6D), and cell size (Figure S6E).

To test whether the SKIP proteins support conditions necessary for proper H2B ubiquitination, we analyzed Lge1 stability, H2B ubiquitination, and H2B-dependent cell morphology when either *At* SKIP or *Hs* SKIP is expressed in *prp45ΔCTR* cells. Indeed, Lge1 levels are increased in *prp45ΔCTR* cells expressing A*t* SKIP or *Hs* SKIP (Figure 6E). Furthermore, when the degron-tagged Prp45 protein is degraded in the presence of IAA, Lge1 protein is lost with similar kinetics as Prp45 degradation (Figure 3C and S6B left image). However, in cells expressing *At* or *Hs* SKIP, Lge1 stability is enhanced, even in the presence of IAA, further emphasizing the stabilizing effect of the SKIP C-terminus (Figure S6B right image). Not surprisingly, H2B ubiquitination (Figure 6F upper and lower image) and WT cell morphology (Figure 6G) are also restored when either *At* SKIP or *Hs* SKIP is expressed in the Prp45ΔCTR cells. Interestingly, trans expression *of At* SKIP and *Hs* SKIP or the C-terminal domain of Prp45 in *the prp45ΔCTR* strain does not significantly increase the levels of Prp45ΔCTR protein (Figure S6F). So, the rescue is not simply due to an increase in the level of the N-terminal portion of Prp45.

The observation that the yeast protein interacting with either the *Arabidopsis* or human SKIP protein supports growth and proper H2B monoubiquitination suggests that these interactions form a surface critical for SKIP activity in H2B ubiquitination. Intriguingly,

SKIP from Arabidopsis is critical for flowering and Histone H2BK120 monoubiquitination,[50] consistent with an evolutionarily conserved role for Prp45/SKIP in H2B ubiquitination. Although SKIP proteins from metazoans diverged from *S. cerevisiae* Prp45 million years ago, the role of the disordered region of the protein, the C-terminus, in protein interactions that are critical for Prp45/SKIP activity has been conserved.

Discussion:

Prp45 is structurally conserved from yeast to humans. While Prp45 in *S. cerevisiae* has been characterized for its role in splicing, its homologs in *Arabidopsis thaliana* and mammals have been shown to play roles in transcriptional events involved in flowering time initiation and transcriptional activation, respectively.[19,20] Here, we show that Prp45 is also involved in extra-spliceosomal regulation of gene expression, particularly H2B monoubiquitination via its C-terminal region, thus providing a mechanism for a direct role for the splicing factor in chromatin modification (Figure 7).

The C-terminal, disordered domain of the protein plays a critical role in this activity.
The Prp45 C-terminus contributes to the Prp45 stability and to its ability to interact with and stabilize other proteins. Although about 50 aa of the C-terminal regions of Prp45 have the propensity to form an alpha-helical structure, which is likely affected by protein interactions, much of the Prp45 protein is highly disordered with an extensive low complexity domain (LCD). LCDs facilitate the formation of biomolecular condensates,[51,52] thus separating specific biochemical functions and coordinating biochemical processes.[53,54,55] Lge1, which interacts with Prp45, is another example of the importance of these highly disordered domains. Approximately 85% of its amino acid residues are in a disordered region (Figure S4A right image), and the disordered nature of Lge1 is critical for Bre1's recruitment to nucleosomes and H2B monoubiquitination.

Studies have shown that WAC (WW domain-containing adaptor with coiled-coil) is the Lge1 homolog in mammals. Similar to the yeast protein, WAC contains an extensive N-

terminal disordered region and a conserved coiled-coil domain.[44]The WAC protein interacts with RNF20/40 through its coiled-coil domain, which is the mammalian homolog of Bre1. The N-terminal WW-containing domain interacts with RNA polymerase II and recruits RNF20/40 for H2B monoubiquitination and transcriptional regulation. H2B monoubiquitination is completely lost upon WAC deletion.[56] In plants, the Bre1 homologs HUB1 and HUB2 are responsible for H2B monoubiquitination, but no Lge1 homolog has been found.[57]

We show that Prp45 provides the structural support for the Lge1. Without Prp45, Lge1 becomes unstable, and cells lose the ability to form Lge1-containing puncta (Figure 4A). As puncta formation is reduced in the *prp45ΔCTR* strain, Bre1 is no longer concentrated in the nucleus and becomes evenly distributed in the cell, as evident from its increased presence in the cytoplasm from the protein transit assay (Figure 4D).

Loss of H2B monoubiquitination in *lge1Δ* and *bre1Δ* cells causes a large-cell phenotype[48] in yeast, which could reflect a defective checkpoint, as in mammalian cells, H2B monoubiquitination is required for effective activation of cell cycle checkpoints during genotoxic stress.[56]

We show that *prp45ΔCTR* cells also exhibit a large, elongated cell phenotype. We also show a significant reduction in H2B monoubiquitination, thus suggesting cell cycle disruption in *prp45ΔCTR* cells could be due to H2B monoubiquitination, but we cannot rule out the possibility of a splicing defect, as Prp45 is also an important splicing factor. In fact, Abramova et al have shown that splicing of some important cell cycle regulators is also inhibited in the *prp45ΔCTR* strain, for example, *ACT1*. We believe it could be the combinatorial effect of both the splicing and H2B monoubiquitination, which leads to increased cell size.

Trans expression of the C-terminal domain not only restores the growth defect and cell size but also restores H2B monoubiquitination and, to a lesser extent, splicing (data not shown), suggesting a unique role for the C-terminal domain. Although the C-terminal domains from Arabidopsis and Human cannot rescue the growth defect, fusing them to

the *S. cerevisiae* N-terminal domain rescues the growth defect and H2B monoubiquitination, suggesting a conserved role of the C-terminal domain in H2B monoubiquitination.

Yeast and metazoan Prp45 proteins do not share any sequence similarity beyond the evolutionarily conserved SNWKN motif (Figure S1). Studies indicate that the SNWKN motif is essential for Prp45 to be part of the spliceosome. Interestingly, trans expression of the C-terminal domain without the SNWKN motif in yeast can slightly improve growth, cell size, and H2B mono ubiquitination but cannot restore splicing (data not shown).

We believe that Prp45 can exist in two different complexes; one form exists in the spliceosome, and the other form exists in the chromatin modification complex. That is why the C-terminal domain without the SNWKN motif cannot restore the splicing defect but moderately restores cell growth, cell size, and H2B monoubiquitination.

An outstanding question is how the interactions described here affect intron-containing genes. The yeast genome architecture provides some hints about how Prp45 may influence chromatin structure and histone modifications at intron-containing genes. Histone H2B monoubiquitination is enriched in highly expressed genes, particularly the ribosomal protein genes that contain introns.[58] Moreover, H2B monoubiquitination marks exon-intron boundaries,[24,59] and splicing of a subset of transcripts is particularly sensitive to this modification. These data suggest that features of the intron-containing genes determine sensitivity to H2B monoubiquitination levels, and further studies are needed to define the internal “logic” of splicing’s dependence or independence from H2B monoubiquitination. Notably, the exon-intron boundary of human genes is also marked by histone H2B monoubiquitination.[60]

It is intriguing to consider the possibility that enrichment of H2B monoubiquitination at some of the most highly expressed genes in the genome, e.g., ribosomal protein genes, the largest class of intron-containing genes, helps coordinate gene expression with cell division, such that, when these processes are dysregulated (for example, by Prp45 truncation), cell division is impaired. The fact that this phenotype is reversed upon *UBP8* deletion reinforces the idea that Prp45’s role in H2B monoubiquitination, at least in part, contributes to cell size homeostasis (Figure 4E).

While the Prp45 affects H2B monoubiquitination through its C-terminal domain and destabilizes lge1, the genetic data point towards broader relationships. If Prp45 solely acts through this pathway, then the synthetic lethality between *prp45*Δ*CTR* and *lge1*Δ would be difficult to explain. Lge1's instability through C-terminal truncation of Prp45 should not have a worse outcome than simply deleting lge1. The same applies to Bre1. Deletion of bre1 or lge1 results in a complete loss of H2B monoubiquitination, although these cells grow like wild-type cells. Interestingly, when these deletions are combined with *prp45*Δ*CTR*, the outcome is synthetic lethal (Figure 2A). This epistasis data suggest that the C-terminal domain might have other functions, probably splicing, in addition to its now-established role in H2B monoubiquitination. We also mentioned earlier that the C-terminal domain is required to maintain the protein's stability per se. Thus, suggesting the multiple roles of the C-terminal domain of Prp45.

When we surveyed the landscape of genetic interactions that are shared between *prp45*Δ*CTR* and *lge1*Δ or *bre1*Δ. Our studies reveal significant overlaps. For example, *set2*Δ is synthetically lethal with *lge1*Δ and *bre1*Δ,[61,30,62,63] a phenotype shared with *prp45*Δ*CTR* (Data not shown). Other gene deletions that lead to synthetically lethal combinations when combined with *bre1*Δ and *lge1*Δ include htz1Δ, swr1Δ, swc3Δ, swc5Δ, and Npl3.[30,64,63,65] These are also synthetically lethal when combined with *prp45*Δ*CTR* (Data not shown[21,58]). Taking, together, these suggest that the role we show here for the Prp45 C-terminus-Lge1/Bre1 interaction is part of a network of chromatin-related functions that are essential for proper cellular function.

Acknowledgements:

AP, TLJ, and the work in the Johnson lab are supported by the NIH (R35GM149290).

We would like to express our gratitude to Dr. Hillery Coller for providing Human Fibroblast cells, and Dr. Jeffrey A. Long for providing *Arabidopsis* leaves for RNA isolation. Thank you also to Drs. Long and Pavak Shah for access to confocal microscopy facilities and for assistance with confocal image analysis. Thank you to Dr. Azad Hossain and members of the Johnson Lab for careful reading of the manuscript.

The authors would like to acknowledge the UCLA Core Mass Spectrometry Facility for their technical support and access to instrumentation.

Figure Legends

Figure 1. Prp45 has a disordered C-terminus that is required for viability at elevated temperatures

(A) Schematic of the domain architecture of the Prp45 protein. The disordered region of the protein was predicted by AIUPred.

(B) The structure of *Sc* PRP45, *At* SKIP, and *Hs* SNW1 protein generated by AlphaFold showing the conserved alpha helical domain.

(C) The C-terminal mutants of Prp45 shows temperature dependent growth defect. Prp45 C-terminal truncated mutants were grown at 30°C and serially diluted on YPD and incubated at 30°C or 37°C (four days each).

Figure 2. The Prp45 C-terminus interacts with the histone ubiquitination machinery

(A) H2B-ub ligase complex deletions (*bre1*Δ, *rad6*Δ, *lge1*Δ) exacerbate *prp45*Δ*CTR* growth defect; deletion of H2B deubiquitinase complex components (*ubp8*Δ and *sgf73*Δ) suppresses it. Cells were serially diluted tenfold, plated on YPD, and grown at 37°C for four days.

(B) Schematic of *in vivo* ubiquitome analysis using WT or *prp45*Δ*CTR* cells. Quantification of ubiquitylated H2BK123 peptides in WT and the *prp45*Δ*CTR* strain was done from the mass spectrometry data.

(C) Truncation of the C-terminal domain of Prp45 causes a significant reduction in H2B monoubiquitination. Immunoblot analysis of ubiquitinated histone H2B in whole-cell extracts isolated from WT and *prp45*Δ*CTR* strains grown at 37°C. Increasing amounts of lysates were loaded onto 15% SDS-PAGE, and ubiquitinated H2B, or H2B, was detected with anti-H2BK123ub or anti-H2B antibodies.

(D) Deletion of UBP8 restores the H2BK123 ubiquitination. H2BK123 monoubiquitination was detected from WCE of WT, *prp45*Δ*CTR,* and *prp45*Δ*CTR ubp8*Δ strains.

Figure 3. The interaction between Prp45 and Lge1 is required for the stability of the Lge1

(A) Prp45 physically interacts with the Lge1. Prp45-HA was immunoprecipitated with Anti-HA antibody and immunoblotted with Anti-FLAG antibody to detect Lge1. 2% of the total lysate was used as an input. Asterisks in lanes 2, 3, 5, and 6 indicate the heavy chains of the primary antibody (top panel) and the light chains (bottom panel left and right).

(B) The loss of the C-terminal domain of Prp45 causes a reduction in Lge1 stability. Immunoblot analysis of whole-cell extracts isolated from WT and *prp45ΔCTR* cells grown at 37°C showed that Lge1-FLAG was detected using an anti-FLAG antibody. Densitometric quantification was done using ImageJ, as shown below. RT-PCR analysis of LGE1 RNA at 37°C shows comparable levels of RNA between the wild type and the *prp45ΔCTR* strain (right image).

(C) The loss of Prp45 protein also causes unstable Lge1 protein. Immunoblot analysis of Lge1 protein upon auxin-inducible degradation of Prp45 when cells were incubated with IAA at different time points (0, 15', 30', and 60'). The DMSO control is shown in lanes 1-4. Prp45-AID-HA and Lge1-FLAG were detected using anti-HA and anti-FLAG antibodies, respectively. Ubiquitinated H2BK123 and H2B were detected using anti-H2BK123-ub and anti-H2B antibodies.

(D) Growth assay illustrating Lge1 instability. Lge1 was N-terminally tagged with a Kanamycin resistance cassette and C-terminally tagged with a degron sequence under the native Lge1 promoter in wild-type and *prp45ΔCTR* strains (schematic). Cells were tenfold serially diluted on a YPD + kanamycin + IAA plate and incubated at 30°C.

Figure 4. Auxin-mediated Prp45 degradation causes Lge1 degradation, which results in altered distribution of Bre1 between the nucleus and cytoplasm

(A) Reduction in Lge1 intensity and puncta formation in the nucleus. The intensity of Lge1-GFP was measured using confocal microscopy at 63X in a strain in which Prp45 was degraded with auxin.

(B) Cell segmentation and intensity quantification. Confocal images of cells treated with or without auxin were segmented to measure cell size and GFP intensity using CellPose. Cell size and GFP intensity were quantified and plotted in the graph.

(C) Distribution of Bre1 is altered between the nucleus and cytoplasm in the *prp45ΔCTR* strain. Bre1 was GFP tagged in WT and *prp45ΔCTR*. Confocal images show the altered distribution of GFP-tagged Bre1 in the *prp45ΔCTR* strain.

(D) Protein transit assay. Immunoblot showing a change in biotinylated Bre1 protein, either by HTZ1 Turbo in the nucleus or PGK1 Turbo in the cytoplasm. The data were quantified and plotted using GraphPad PRISM.

(E) The large cell size of the *prp45ΔCTR* strain was restored by the deletion of UBP8. Confocal imaging (DIC) of WT, *prp45ΔCTR,* and *prp45ΔCTR ubp8Δ* strains grown to OD_{600} 0.6 at 37°C was done, and cell size was measured using ImageJ. Cell size (n = 80) was plotted in GraphPad PRISM, and an unpaired one-way ANOVA with Tukey's post hoc test was used to calculate *p*-values.

Figure 5. Trans expression of the C-terminal domain of Prp45 rescues cell growth, H2B ubiquitination, Lge1 stability, and cell morphology.

(A) The trans expression of the C-terminal domain rescues the growth defect at high temperature. WT, *prp45ΔCTR*, *prp45ΔCTR* + the C-terminal domain (175-379) of Prp45, and *prp45ΔCTR* + the C-terminal domain (170-379) of Prp45 expressed from a plasmid (pRS315) were grown in Sc-Leu media. Cells were serially diluted tenfold and incubated at 37°C for six days.

(B) Growth assay illustrating Lge1 stability in trans expressed C-terminal domain of Prp45 in *prp45ΔCTR* strains. Lge1 was N-terminally tagged with a Kanamycin resistance cassette and C-terminally tagged with a degron sequence under the native Lge1 promoter in wild-type, *prp45ΔCTR,* and *prp45ΔCTR* + the C-terminal domain of Prp45 strains. Cells were tenfold serially diluted on a YPD + kanamycin + IAA plate and incubated at 30°C.

(C) Trans expression of the C-terminal domain restores the stability of the Lge1 protein. Immunoblot analysis of whole cell extracts isolated from WT, *prp45ΔCTR*, and *prp45ΔCTR* + plasmid-borne C-terminal domain of Prp45 was done; Lge1-FLAG was detected using anti-FLAG antibody. H2B was used as a loading control, and densitometric quantification was done using ImageJ, as shown below.

(D) Immunoblot of whole cell extracts isolated from WT, *prp45ΔCTR*, *prp45ΔCTR* + C-terminal (175-379) and (170-379) domain of Prp45 was done, H2BK123 ubiquitination

and H2B were detected using anti-H2BK123 and anti-H2B antibodies. Densitometric quantification was done using ImageJ, as shown below.

(E) (Left) Confocal imaging of WT, *prp45ΔCTR,* and *prp45*ΔCTR + plasmid-borne C-terminal domain (175-379) and (170-379) of Prp45 strains grown to OD_{600} 0.6 at 37°C (Right) *p*-values from unpaired one-way ANOVA with Tukey post hoc analysis; n = 80.

Figure 6. The function of Prp45 C-terminus is evolutionarily conserved

(A) The C-terminal regions of Prp45 from *S cerevisiae*, *Arabidopsis thaliana*, and *Homo sapiens* were expressed in *the prp45ΔCTR* strain, showing that only the *Sc* C-terminus could rescue the growth defect (upper growth assay image). The fusion between *At* C-SKIP and the *Sc* Prp45 N-terminus (1-169), i.e., the chimera, can rescue the growth defect (middle growth assay image). Trans expression of full-length *At* SKIP or *Hs* SKIP in *prp45ΔCTR* strain could rescue the growth defect at 37°C (lower growth assay image).

(B) Growth assay showing Lge1 stability, at 30°C in the chimera strain. Lge1 was N-terminally tagged with a Kanamycin resistance cassette and C-terminally tagged with a degron sequence under the native Lge1 promoter in wild type, *prp45ΔCTR* and *Sc_At PRP45* chimera strains. Cells were tenfold serially diluted on a YPD + kanamycin + IAA plate and incubated at 30°C.

(C) The chimera can restore H2B monoubiquitination. A Immunoblot of whole cell extracts isolated from WT, *prp45ΔCTR,* and *Sc_At PRP45* chimera strains was performed; H2BK123 ubiquitination and H2B were detected using anti-H2BK123 and anti-H2B antibodies.

(D) Chimera restores the cell size. Confocal imaging (DIC) of WT, *prp45ΔCTR,* and *Sc_At PRP45* chimera strains grown to OD_{600} 0.6 at 37°C was done, and cell size was measured using ImageJ. Cell size was plotted in the graph using GraphPad PRISM, and an unpaired one-way ANOVA with Tukey's post hoc analysis (n = 80) was used to calculate the *p*-values.

(E) Trans expression of *At* SKIP and *Hs* SKIP restores Lge1 stability. Whole-cell extracts from the respective strains were isolated, and an immunoblot was performed to assess changes in Lge1 stability in *prp45ΔCTR* strains expressing *At* SKIP or *Hs* SKIP.

(F) *At* and *Hs* SKIP and *Sc_At* chimera can rescue the H2B monoubiquitination. Immunoblot of whole cell extracts isolated from WT, *prp45ΔCTR,* and *prp45ΔCTR* strains expressing *At* SKIP or *Hs* SKIP (Upper and lower image) and *Sc-At* chimera was done, H2BK123 ubiquitination and H2B were detected using anti-H2BK123 and anti-H2B antibodies.

(G) *At* and *Hs* SKIP also restore the cell size. Confocal imaging (DIC) of WT, *prp45ΔCTR,* and *prp45ΔCTR* strains expressing *At* SKIP or *Hs* SKIP grown to OD_{600} 0.6 at 37°C was done, and cell size was measured using ImageJ. Cell size was plotted in the graph using GraphPad PRISM, and an unpaired one-way ANOVA with Tukey's post hoc analysis (n = 80) was used to calculate the *p*-values.

Figure 7. Model of Prp45 effects on histone H2B ubiquitination.

The model shows that truncation of the C-terminal domain or partial degradation of the Prp45 protein (orange) renders the Lge1 protein (light blue) unstable. The biomolecular condensate formed by the Lge1 protein is also significantly reduced as a result; Lge1 can no longer concentrate Bre1 (dark blue) in the nucleus. The distribution of the Bre1 protein is altered between the nucleus and cytoplasm.

Supplementary Figure 1. **Prp45 and its homolog's Sequence alignment**

(A) Sequence alignment. UniProt IDs were used to retrieve the sequences of Prp45 from *S. cerevisiae*, *Arabidopsis thaliana*, and *Homo sapiens*; sequence alignment was performed using ClustalW.

Supplementary Figure 2. The C-terminal region-specific interactors of Prp45 identified by in vivo biotinylation and loss of the C-terminal domain also affect its stability

(A) Schematic of the *in vivo* biotinylation assay, where full-length Prp45 and Prp45ΔCTR are C-terminally Biotin ligase tagged.

(B) Interactors identified from mass spectrometry data. The Venn diagram indicates 38 unique interactors specific to the full-length Prp45 only and 213 interactions that occur with both

(C) Hierarchical clustering of the interactors that show a significant change in interaction with Prp45 FL and Prp45ΔCTR. BRR2, SPP2, PRP46, CLF1, PRP45, CBF1, TRM82, and HSP12 show a significant reduction in interaction when the C-terminal end of Prp45 is deleted.

Supplementary Figure 3. The C-terminal domain is required to maintain the optimal stability of the Prp45 protein

(A) Immunoblot showing the changes in the stability of Prp45 protein and Prp45ΔCTR protein at 37°C, whereas RNA expression remained unchanged (right gel image).

(B) C-terminal domain protects Prp45 from degradation at high temperatures. Prp45 and Prp45ΔCTR were degron-tagged and grown on YPD + IAA at 30°C and 37°C for 4 days. This assay shows that the C-terminal domain is required to maintain the stability of the Prp45 protein.

(C) Deletion of UBP8 does not rescue the stability of Prp45ΔCTR protein. Immunoblot analysis of whole cell extracts isolated from WT, *prp45ΔCTR,* and *prp45ΔCTR ubp8Δ* cells grown at 37°C, and the stability of Prp45 and Prp45ΔCTR protein was checked in those above-mentioned strains using anti-HA antibody.

(D) Growth assay showing another role of Prp45 apart from its role in H2B monoubiquitination. Deletion of UBP8 in *the prp45ΔCTR* strain can rescue the growth defect, but it cannot rescue the growth defect in *the prp45ΔCTR* Degron strain, as the whole Prp45 protein is degraded. WT, *prp45ΔCTR Degron,* and UBP8 deleted *prp45ΔCTR* Degron strains were grown in YPD at 30°C and then 10- fold serially diluted on YPD + IAA plate and incubated at 30°C or 37°C for four days.

Table S1: List of proteins that show Prp45's C-terminal domain-specific interaction, and the interaction is lost when the C-terminal domain is truncated. Proteins were grouped based on their association with the major pathway complexes.

Supplementary Figure 4. The coiled-coiled domain of Lge1 shows synthetic genetic interaction with *prp45ΔCTR*

(A) (Left) *In silico* Prp45 (purple) and Lge1 (orange) interaction analysis by AlphaFold multimer and visualized in Chimera X. The cyan color shows the interaction sites, especially at the C-terminal region of Prp45, with the Lge1.

(Right) The disordered and structural domains of the Lge1 protein were mapped using Metapredict. The dark shaded region indicates the disorder region, and the region from `270 to 332 is the ordered region. The sharp decrease and increase in the red and blue lines indicate that the region is more structured and a site for potential protein interaction.

(B) Deletion of the CC domain of Lge1 causes loss of H2B monoubiquitination. Whole cell lysates isolated from WT, *lge1ΔCC,* and *bre1Δ* grown at 30°C and analyzed by Immunoblot for the detection of H2BK123 monoubiquitination and H2B using anti-H2BK123ub and anti-H2B antibodies.

(C) CC deleted Lge1 shows a synthetic lethal genetic interaction with *prp45ΔCTR.* WT, *prp45ΔCTR*, *prp45ΔCTR lge1Δ*, *prp45ΔCTR lge1ΔCC,* and *lge1ΔCC* cells were grown in YPD, tenfold serially diluted on a YPD plate, and incubated at 30°C or 37°C for four days.

(D) CC deleted lge1 also shows large phenotypes. Confocal imaging (DIC) of WT, *prp45ΔCTR,* and *lge1Δ* strains grown to OD_{600} 0.6 at 37°C was done, and cell size was measured using ImageJ. Cell size was plotted in the graph using GraphPad PRISM,

unpaired one-way ANOVA with Tukey post hoc analysis; n = 80, was done for calculating the *p*-values.

Supplementary Figure 5. The genomic retention of the disordered region of Prp45 (1-260) interacts with the H2B ubiquitination machinery

(A) The genomic truncation after the disordered region (1-260) of Prp45 restores the stability of Prp45. Whole cell lysates isolated from WT, *prp45ΔCTR,* and *prp45 (1-260)*, grown at 37°C, and analyzed by Immunoblot for the detection of Prp45, Prp45ΔCTR, and Prp45 (1-260) protein using anti-HA antibody.
(B) Growth assay showing Lge1 stability, in Prp45(1-260) strain. Lge1 was N-terminally tagged with a Kanamycin resistance cassette and C-terminally tagged with a degron sequence under the native Lge1 promoter in wild type, *prp45ΔCTR* and *prp45 (1-260)* strains. Cells were tenfold serially diluted on a YPD + kanamycin + IAA plate and incubated at 30°C.
(C) Prp45 (1-260) rescues H2B monoubiquitination. Whole cell lysates isolated from WT, *prp45ΔCTR,* and *prp45 (1-260)*, grown at 37°C, and analyzed by Immunoblot for the detection of H2BK123ub and H2B using anti-H2BK123ub and H2B antibodies.
(D) Prp45 (1-260) also restores the large cell morphology. Confocal imaging (DIC) of WT, *prp45ΔCTR,* and *prp45 (1-260)* strains grown to OD_{600} 0.6 at 37°C was done, and cell size was measured using ImageJ. Cell size was plotted in the graph using GraphPad PRISM, and an unpaired one-way ANOVA with Tukey's post hoc analysis (n = 80) was used to calculate the *p*-values.

Supplementary Figure 6. **Prp45 homologs from metazoans also become part of the H2B ubiquitination machinery when expressed in *S cerevisiae***
(A) Different truncation mutants of the C-terminal domain of Prp45 and trans-expressed *At* or *Hs* SKIP cannot rescue the growth defect in *prp45Δ. prp45Δ* + pRS315 (PRP45), *prp45ΔC* + pRS316 (PRP45), *prp45Δ* + pRS315 (170-379), *prp45Δ* + pRS315 (175-379), *prp45Δ* + pRS315 (184-296), *prp45Δ* + pRS315 (*At* SKIP), *prp45Δ* + pRS315 (*Hs* SKIP)

cells were grown in SC-URA, tenfold serially diluted on SC FOA -URA, and incubated at 30°C for five days.

(B) Trans expression of *At* and *Hs* SKIP in Prp45 degron not only prevents the degradation of Lge1 but also the Sc Prp45. Immunoblot analysis of Lge1 protein upon auxin-inducible degradation of Prp45 when cells were incubated with IAA at different time points (0, 15' and 30') (left gel image).

Immunoblot analysis of Lge1 protein upon auxin-mediated degradation of degron-tagged *Sc* Prp45 in the presence of *At* SKIP and *Hs* SKIP (right gel image) also shows the expression of *At* SKIP and *Hs* SKIP.

(C) *Sc_Hs* chimeric Prp45 rescues the growth defect.

(D) Human chimera can restore H2B monoubiquitination and fusing the C-terminal half of Human SKIP protein with the N-terminal half of *Sc* Prp45 restores the stability. Whole cell lysates isolated from WT, *prp45ΔCTR,* and *Sc_Hs* chimera grown at 37°C and analyzed by Immunoblot for the detection of *Sc_Hs* chimera-HA, H2BK123 monoubiquitination, and H2B using anti-HA, anti-H2BK123ub, and anti-H2B antibodies.

(E) *Sc_Hs* chimeric Prp45 rescues the cell size. Confocal imaging (DIC) of WT, *prp45ΔCTR,* and *Sc_Hs* chimera grown to OD_{600} 0.6 at 37°C was done, and cell size was measured using ImageJ. Cell size was plotted in the graph using GraphPad PRISM, and an unpaired one-way ANOVA with Tukey's post hoc analysis (n = 80) was used to calculate the *p*-values.

(F) The trans expression of Sc C-terminal domain or *At* SKIP/*Hs* SKIP cannot restore the stability of Prp45ΔCTR protein. An immunoblot was done to see if the stability of Prp45ΔCTR HA protein in *prp45ΔCTR, prp45ΔCTR* + trans C-terminal domain, *prp45ΔCTR* + *At* SKIP, and *prp45ΔCTR* + *Hs* SKIP was rescued as compared to the wild-type full-length Prp45 HA protein.

(G) The Chimera protein becomes stable even at high temperatures as compared to the Prp45ΔCTR protein. Whole cell lysates isolated from WT, *prp45ΔCTR,* and *Sc_At* chimera grown at 37°C and analyzed by Immunoblot for the detection of *Sc_At* chimera-HA, H2BK123 monoubiquitination, and H2B using anti-HA, anti-H2BK123ub, and anti-H2B antibodies.

Materials and Methods

Strains and growth conditions:

All strains of *S. cerevisiae* used in this study are listed in Table S1. All strains are derived from BY4741. The Prp45 degron strain was generated by integrating Adh1/AtTIR1 into the HIS3 locus. AID-HA-Hyg was added to the C-terminal of endogenous Prp45 by standard replacement with a marker cassette.[66] Endogenous C-terminal tagged strains were generated by homologous recombination followed by PCR amplification from the pFA6a-3HA-kanMX6 and pFA6a-5FLAG-NatMX6 plasmids as described previously.[66] *Lge1*, *UBP8*, *UBP10*, and *Bre1* were knocked out by replacing the KanMX6 cassette. The C-terminal domain (amino acids 170-379, 175-379, and 184-296) of Prp45, along with the promoter sequence, was PCR-amplified with CloneAmp (Takara) using primers listed in the supplementary material. PCR was performed for 35 cycles, with denaturation at 98°C for 15 seconds, extension at 55°C for 15 seconds, and a final extension at 72°C for 20 seconds. The C-terminal domain or the full length of *At* SKIP and *Hs* SKIP were cloned under *Sc* Prp45's promoter sequence. Amplicon was run on 1.8% agarose gel and gel-purified using the Qiagen gel extraction kit. The purified amplicon was subjected to restriction digestion with *BamHI* and *SalI* and cloned in *BamHI* and *SalI* restriction sites in pRS315 vector (Addgene). The chimeric Prp45 was generated by using primers used to amplify the C-terminal region of *At* SKIP, and the homologous recombination technique was used to integrate it into the yeast genome. Cells were grown on YPD (1% yeast extract, 2% peptone, and 2% glucose) or synthetic dropout media at 30°C and 37°C.

Growth assay:

5mL overnight cultures were transferred to a fresh 50mL YPD or selective dropout media (SC-URA or SC-Leu) and grown at 30°C until the OD reached 0.5. Cells were tenfold serially diluted and spotted on YPD or YPD + Kan + IAA or SC-Leu or SC FOA-URA plates. Plates were kept at 30°C and 37°C to observe the effect of elevated temperature.

In vivo depletion of Prp45 and Lge1:

Prp45-AID-HA and Lge1 AID-HA strains were grown on YPD at 30°C for 1.5 hours, followed by 1mM IAA (I5148, sigma) treatment for different time points. Cells were spun, and the pellets were kept at -80 °C.

Yeast nuclear extract preparation and Immunoblotting:

Saturated overnight 5mL cultures were transferred to 50 mL and allowed to grow at 30°C until they reached an OD of 0.8-1. For elevated-temperature stress, cells were first grown at 30°C for 1 hour, then transferred to 37°C and grown for 2 hours. Cells were pelleted and resuspended in 500μL of lysis buffer (50mM HEPES, pH 7.5, 150mM NaCl, 1mM EDTA, 1% Triton X-100, 0.1% sodium deoxycholate) with protease inhibitor. An equal volume of 0.5 mm acid-washed glass beads (BioSpec) was added to the cell resuspension, and the samples were lysed in a cell disruptor for 10 minutes at 4ºC. Proteins were separated in an 8% SDS-PAGE for Lge1-FLAG, Prp45AID-HA, and a 15% SDS-PAGE for histone H2BK123 monoubiquitination and histone H2B. HA blots were probed with anti-HA antibody (clone 12CA5, Roche), FLAG blots were probed with anti-FLAG antibody (Sigma, catalog no F1804), histone H2BK123Ub1 blots were probed with anti-H2BK123Ub1(anti-ubiquity H2B,5546S; CST, Cell Signaling Technology, Danvers, MA, USA), and histone H2B blots were probed with anti-H2B (Active motif, catalog no 39210). Immunoblots were quantified using ImageJ software.

RNA isolation:

Yeast cells were grown until the A_{600} = 1.0. Total RNA was isolated using the hot acid phenol method. Yeast cells were treated with acidic phenol (P4682; Sigma) at 65 °C, and the RNA was extracted with phenol/chloroform/isoamyl alcohol with SDS, followed by ethanol precipitation. Following total RNA isolation, 25μg of RNA was treated with DNase I (Roche). 3μg of DNase I-treated RNA was used for cDNA synthesis. The first strand of cDNA was generated using Maxima Reverse Transcriptase (ThermoFisher Scientific). Gene-specific primers are listed in the supplementary material table S1. 1–2 μL of cDNA was used as the template in a 25 μL PCR reaction.

Co-immunoprecipitation:

25mL overnight saturated culture was transferred to 125mL of fresh YPD, and cells were grown until A_{600}=0.8-1. Cells were then pelleted and resuspended in 1mL of lysis buffer with protease inhibitors. Acid-washed beads were added to the resuspension, and samples were lysed in a cell disruptor for 10 minutes (one minute ON, one minute OFF) at 4ºC. The lysates were centrifuged at 13,000 rpm for 15 minutes at 4 °C to remove insoluble material.

1 mL of lysate was precleared with 50μL of Protein A/G agarose beads (sc-2003, Santa Cruz Biotechnology). 25μL of precleared lysate was removed as input. 4μg of anti-HA antibody (clone: 12CA5, Roche) was added to the 700μL of clarified lysate and rotated at 4°C overnight. Samples were incubated with 50 μL of Protein A/G agarose beads for 2 hours at 4°C. Beads were then washed five times with lysis buffer and eluted by boiling in 2X SDS-PAGE loading buffer.

Proximity labeling, biotinylation, and Mass-spectrometry:

5 mL TurboID-tagged (Biotin ligase) overnight cultures were transferred to fresh 50mL YPD supplemented with 50 μM biotin. Cells were grown at 30°C until the cultures reached an OD of 0.8. Cell pellets were resuspended in 250μL of RIPA buffer (50mM Tris-HCl, pH 7.5, 150mM NaCl, 1.5mM $MgCl_2$, 1mM EGTA, 0.1% SDS, 1% NP-40, supplemented with 0.4% sodium deoxycholate, 1mM DTT, 1mM PMSF, and 1x complete). Acid-washed beads were added to the resuspension, and samples were lysed in a cell disruptor for 10 minutes at 4°C. The lysates were centrifuged at 13,000 rpm for 15 minutes at 4 °C to remove insoluble material. Lysates were briefly sonicated and treated with benzonase (Medchem exp) for 3 hours at 4°C to digest DNA and RNA. 10mg of total proteins were subjected to affinity purification using 50μL streptavidin (GE) at 4°C for 3 hours. Beads were then washed once with wash buffer (50mM Tris-HCl pH 7.5, 2% SDS) followed by three times wash with RIPA buffer containing DTT (50mM Tris-HCl pH 7.5, 150mM NaCl, 1.5mM $MgCl_2$, 1mM EGTA, 0.1% SDS, 1% NP-40, 1mM DTT). Finally, the beads were washed five times with 20mM ammonium bicarbonate. All the washes were done for 5 minutes at room temperature in a nutator. For mass spectrometric analysis, streptavidin-

bound proteins were reduced with 10 mM DTT, followed by alkylation with 15 mM iodoacetamide.

Protein-bound beads were subjected to trypsin digestion at 37°C overnight, then stopped by the addition of formic acid (final concentration 1%). Peptides were then extracted with acetonitrile, lyophilized, and resuspended in 0.1% trifluoroacetic acid (TFA) for desalting on ZipTips. (EMD Millipore) The cleanup of peptide samples was performed as described previously.[67] Trypsin-digested samples were analyzed by LC/MS. The MaxQuant software package version 1.5.1.2 was used to analyze the data against the S. cerevisiae UniProt proteome. The peak intensity of peptides was used for relative quantification of proteins.

Modified Protein transit assay:

Nuclear protein (HTZ1) and cytoplasmic protein (PGK1) were C-terminally tagged with Turbo ID (biotin ligase) by homologous recombination, followed by PCR amplification from the pFA6a-Turbo-ID-3 Myc-kanMX6. 5 mL TurboID-tagged overnight cultures were transferred to fresh 50mL YPD supplemented with 50 μM biotin. Cells were grown at 30°C until the cultures reached an OD of 0.8. Cell pellets were resuspended in 250μL of RIPA buffer (50mM Tris-HCl, pH 7.5, 150mM NaCl, 1.5mM $MgCl_2$, 1mM EGTA, 0.1% SDS, 1% NP-40, supplemented with 0.4% sodium deoxycholate, 1mM DTT, 1mM PMSF, and 1x complete). Acid-washed beads were added to the resuspension, and samples were lysed in a cell disruptor for 10 minutes at 4°C. The lysates were centrifuged at 13,000 rpm for 15 minutes at 4 °C to remove insoluble material. Lysates were briefly sonicated and treated with benzonase (Medchem exp) for 3 hours at 4°C to digest DNA and RNA. 30mg of total proteins were subjected to affinity purification using 50μL streptavidin (GE) at 4°C for 3 hours. Beads were then washed once with wash buffer (50mM Tris-HCl pH 7.5, 2% SDS) followed by three times wash with RIPA buffer containing DTT (50mM Tris-HCl pH 7.5, 150mM NaCl, 1.5mM $MgCl_2$, 1mM EGTA, 0.1% SDS, 1% NP-40, 1mM DTT). Finally, the beads were washed five times with 20mM ammonium bicarbonate. All the washes were done for 5 minutes at room temperature in a nutator. Beads were then washed twice with lysis buffer and eluted by boiling in 2X SDS-PAGE loading buffer.

***In silico* protein interaction analysis:**

Alphafold2 was used to generate three-dimensional protein structures, and Google Colabfold was used to analyze the protein-protein interaction. The best fit model was fetched to ChimeraX 1.9, and subsequent analysis was done in ChimeraX 1.9, including probable contact sites between the interacting proteins.

Microscopy and image quantification:

Wild type and mutant strains were stained with 5μM DAPI and observed under the 63X oil immersion lens. The images were quantified using ImageJ. Cell counting and segmentation was done using cell pose. In house MATLAB code was used to analyze and quantify the images.

Statistical analysis:

All experiments were performed a minimum of three times. Statistics in this study were presented as mean ± SD. Error bars represented SD in triplicate experiments. Statistical significance (*p*-values) for comparison was assessed by One-way ANOVA with Tukey post-hoc analysis.

Supplementary Material

Genotype	Source
MATa his3Δ1 leu2Δ0 met15Δ0 ura3Δ0 (WT)	Open Biosystems
MATa PRP45-HA::KANMX6 his3Δ1 leu2Δ0 met15Δ0 ura3Δ0	This study
MATa PRP45ΔCTR-HA::KANMX6 his3Δ1 leu2Δ0 met15Δ0 ura3Δ0	This study
MATa PRP45-HA::KANMX6 Lge1-FLAG::NATMX6 his3Δ1 leu2Δ0 met15Δ0 ura3Δ0	This study
MATa PRP45ΔCTR-HA::KANMX6 Lge1-FLAG::NATMX6 his3Δ1 leu2Δ0 met15Δ0 ura3Δ0	This study
MATa PRP45-HA::KANMX6 Lge1ΔCC-FLAG::NATMX6 his3Δ1 leu2Δ0 met15Δ0 ura3Δ0	This study
MATa PRP45(1-174)-HA::KANMX6 his3Δ1 leu2Δ0 met15Δ0 ura3Δ0	This study
MATa PRP45(1-184)-HA::KANMX6 his3Δ1 leu2Δ0 met15Δ0 ura3Δ0	This study
MATa PRP45(1-260)-HA::KANMX6 his3Δ1 leu2Δ0 met15Δ0 ura3Δ0	This study
MATa PRP45(1-296)-HA::KANMX6 his3Δ1 leu2Δ0 met15Δ0 ura3Δ0	This study
MATa Bre1-GFP::KANMX6 his3Δ1 leu2Δ0 met15Δ0 ura3Δ0	This study
MATa Bre1-GFP::KANMX6 PRP45ΔCTR-FLAG::NATMX6 his3Δ1 leu2Δ0 met15Δ0 ura3Δ0	This study
MATa UBP8Δ-FLAG::NATMX6 his3Δ1 leu2Δ0 met15Δ0 ura3Δ0	Open Biosystems
MATa UBP8Δ-FLAG::NATMX6 PRP45ΔCTR-HA::KANMX6 his3Δ1 leu2Δ0 met15Δ0 ura3Δ0	This study
MATa UBP10Δ-FLAG::NATMX6 PRP45ΔCTR-HA::KANMX6 his3Δ1 leu2Δ0 met15Δ0 ura3Δ0	This study

MATa LGE1Δ-FLAG::NATMX6 PRP45ΔCTR-HA::KANMX6 his3Δ1 leu2Δ0 met15Δ0 ura3Δ0	This study
MATa LGE1ΔCC-FLAG::NATMX6 PRP45-HA::KANMX6 his3Δ1 leu2Δ0 met15Δ0 ura3Δ0	This study
MATa LGE1ΔCC-FLAG::NATMX6 PRP45ΔCTR-HA::KANMX6 his3Δ1 leu2Δ0 met15Δ0 ura3Δ0	This study
MATa LGE1Δ-FLAG::NATMX6 his3Δ1 leu2Δ0 met15Δ0 ura3Δ0	Open Biosystems
MATa BRE1Δ-FLAG::NATMX6 his3Δ1 leu2Δ0 met15Δ0 ura3Δ0	Open Biosystems
MATa BRE1Δ-FLAG::NATMX6 PRP45ΔCTR-HA::KANMX6 his3Δ1 leu2Δ0 met15Δ0 ura3Δ0	This study
MATa RAD6Δ-FLAG::NATMX6 his3Δ1 leu2Δ0 met15Δ0 ura3Δ0	Open Biosystems
MATa RAD6Δ-FLAG::NATMX6 PRP45ΔCTR-HA::KANMX6 his3Δ1 leu2Δ0 met15Δ0 ura3Δ0	This study
MATa PRP45-AID-HA::Hyg LGE1-FLAG:NATMX6 his3Δ1 leu2Δ0 met15Δ0 ura3Δ0	This study
MATa SGF73Δ-FLAG::NATMX6 PRP45ΔCTR-HA::KANMX6 his3Δ1 leu2Δ0 met15Δ0 ura3Δ0	This study
MATa SGF73Δ-FLAG::NATMX6 his3Δ1 leu2Δ0 met15Δ0 ura3Δ0	Open Biosystems

Primer name	Sequence (5' to 3')	Purpose
SCR1 F	AAGGGATAGTTCTCTATTCCGCACC	RT-PCR
SCR1 R	CACAATGTGCGAGTAAATCCTGATG	RT-PCR
Prp45 (Stitching forward primer promoter-300bp)	ACG CGA GGA TCC TCG ACC GGG CAT AGA ATA GC	Cloning
Stitching reverse primer promoter and ATG of Prp45	GGA TTT TTC CAG TTT GAC ATA TTT GGT TGA GGT	Cloning

Stitching forward primer for C-terminal end of Prp45	ACC TCA ACC AAA TAT GTC AAA CTG GAA AAA TCC	Cloning
Prp45 C- terminal stitching with FLAG sequence reverse primer	CGT CGT CCT TGT AGT C GGC GCC ATA GTT ATC CG	Cloning
Prp45 C- terminal stitching with FLAG sequence Forward primer	CGG ATA ACT ATG GCG CC GAC TAC AAG GAC GAC G	Cloning
FLAG sequence + ADH1 terminator reverse primer	TTG GCC GTC GAC CCG GTA GAG GTG TGG TCA AT	Cloning
Prp45 (1-169) F	AGA AGC TGA TCC AAA TGA GTG GAA GAT ACC TGC AGC TGT G CGGATCCCCGGGTTAATTAA	Deletion & tagging
Prp45 (1-169) R	CCA AGG CCA CGG TAT AAC CAT TTG GAT TTT TCC AGT TTG A GAATTCGAGCTCGTTTAAAC	Deletion & tagging
Prp45 (1-260) F	AGC CAG ATA CCA CAA CGG GAC TCC GCA GAC GGG AGC AAT A CGGATCCCCGGGTTAATTAA	Deletion & tagging
Prp45 (1-260) R	TTA GTC TGG CCA CTG TGC TCG TTT GCT TTT TGG GCT TAA C GAATTCGAGCTCGTTTAAAC	Deletion & tagging
UBP8 deletion F	GTA ATA GCA AAG GGA TTA TAT TAG TGG ACC TGA TTA ATT C CG GAT CCC CGG GTT AAT TAA	deletion
UBP8 deletion R	TAT AGA AAA AAG AAC GGA AGC AAG CGT TAA CTG TGA TAG G GAATTCGAGCTCGTTTAAAC	deletion
BRE1 deletion F	GCA TTT GAT CAC GTG ATT ATA ATC ACA TCC AAC GAA AC CG GAT CCC CGG GTT AAT TAA	deletion
BRE1 deletion R	TAG ACG TCA CTC TTT GAT TCA GAA GTT AGG CTA GGA TG GAATTCGAGCTCGTTTAAAC	deletion

SGF73 deletion F	AAA ATC ATT ACG AAC AGA AGA AAG TGG AGC TGA AGA GCG T CG GAT CCC CGG GTT AAT TAA	deletion
SGF73 deletion R	TGA AGA AAT ATA ATG TCT ACT TAA ATA AAT AAT GTA TAC C GAATTCGAGCTCGTTTAAAC	deletion
RAD6 deletion F	ATA TAC AAA AAG GCA CCT CCG GGT AGC CGG AGT AGA AAG C CG GAT CCC CGG GTT AAT TAA	deletion
RAD6 deletion R	GAA TTC ATA ATA TCG GCT CGG CAT TCA TCA TTA AGA TTC T GAATTCGAGCTCGTTTAAAC	deletion
LGE1 C-terminal tagging F	ACT GAC CCA AGA AAA GCT GGA CTC ATT GTT ATT AAT GCA G CG GAT CCC CGG GTT AAT TAA	tagging
LGE1 C-terminal tagging R	TGC GTT TAC GTA GTT TAT CTA TTT ATA GGT ACG GTA TAC C GAATTCGAGCTCGTTTAAAC	tagging
PRP45 degron F	TAA AGCTGAATCC GATGATAAAT CGGATAACTA TGGCGCC CG TAC GCT GCA GGT CGA C	tagging
PRP45 degron R	AGCACAAGAATGCTTTGTTTTCCTAGTGCTCATCCTGGGCATC GAT GAA TTC GAG CTC G	tagging
Prp45 (1-169) degron F	AGA AGC TGA TCC AAA TGA GTG GAA GAT ACC TGC AGC TGT G CGT ACG CTG CAG GTC GAC	tagging
Prp45 (1-169) degron R	CCA AGG CCA CGG TAT AAC CAT TTG GAT TTT TCC AGT TTG A ATC GAT GAA TTC GAG CTC G	tagging
Lge1 degron F	ACT GAC CCA AGA AAA GCT GGA CTC ATT GTT ATT AAT GCA G CGT ACG CTG CAG GTC GAC	tagging
Lge1 degron R	TGC GTT TAC GTA GTT TAT CTA TTT ATA GGT ACG GTA TAC C ATC GAT GAA TTC GAG CTC G	tagging
HTZ1 C-terminal Turbo ID tagging F	AGC ATT ATT ATT GAA AGT GGA AAA AAA GGG AAG TAA GAA A CG GAT CCC CGG GTT AAT TAA	Tagging

HTZ1 C-terminal Turbo ID tagging F	AGG GAG AAT TAC GGG AAA TGG GAA AGA AAA ACT ATT CTT C GAATTCGAGCTCGTTTAAAC	tagging
PGK1 C-terminal Turbo ID tagging F	TAA GGA ATT GCC AGG TGT TGC TTT CTT ATC CGA AAA GAA A CG GAT CCC CGG GTT AAT TAA	
PGK1 C-terminal Turbo ID tagging R	AAA GAA AAA AAT TGA TCT ATC GAT TTC AAT TCA ATT CAA T GAATTCGAGCTCGTTTAAAC	

References Cited

1. Cheng, S.C., and Abelson, J. (1987). Spliceosome assembly in yeast. Genes Dev *1*, 1014–1027. 10.1101/gad.1.9.1014.
2. Chan, S.-P., Kao, D.-I., Tsai, W.-Y., and Cheng, S.-C. (2003). The Prp19p-associated complex in spliceosome activation. Science *302*, 279–282.
3. Albers, M., Diment, A., Muraru, M., Russell, C.S., and Beggs, J.D. (2003). Identification and characterization of Prp45p and Prp46p, essential pre-mRNA splicing factors. Rna *9*, 138–150. 10.1261/rna.2119903.
4. Chanarat, S., and Sträßer, K. (2013). Splicing and beyond: The many faces of the Prp19 complex. Biochimica et Biophysica Acta (BBA) - Molecular Cell Research *1833*, 2126–2134. https://doi.org/10.1016/j.bbamcr.2013.05.023.
5. Yan, C., Wan, R., Bai, R., Huang, G., and Shi, Y. (2016). Structure of a yeast activated spliceosome at 3.5 Å resolution. Science *353*, 904–911. 10.1126/science.aag0291.
6. Wan, R., Yan, C., Bai, R., Huang, G., and Shi, Y. (2016). Structure of a yeast catalytic step I spliceosome at 3.4 Å resolution. Science *353*, 895–904. 10.1126/science.aag2235.
7. Martinkova, K., Lebduska, P., Skruzny, M., Folk, P., and Puta, F. (2002). Functional Mapping of Saccharomyces cerevisiae Prp45 Identifies the SNW Domain as Essential for Viability. Journal of biochemistry *132*, 557–563. 10.1093/oxfordjournals.jbchem.a003257.
8. Hálová, M., Gahura, O., Převorovský, M., Cit, Z., Novotný, M., Valentová, A., Abrhámová, K., Půta, F., and Folk, P. (2017). Nineteen complex-related factor Prp45 is required for the early stages of cotranscriptional spliceosome assembly. Rna *23*, 1512–1524. 10.1261/rna.061986.117.
9. Gahura, O., Abrhámová, K., Skružný, M., Valentová, A., Munzarová, V., Folk, P., and Půta, F. (2009). Prp45 affects Prp22 partition in spliceosomal complexes and splicing efficiency of non-consensus substrates. Journal of Cellular Biochemistry *106*, 139–151. https://doi.org/10.1002/jcb.21989.
10. Venkatesh, S., and Workman, J.L. (2013). Set2 mediated H3 lysine 36 methylation: regulation of transcription elongation and implications in organismal development. Wiley Interdiscip Rev Dev Biol *2*, 685–700. 10.1002/wdev.109.
11. DiFiore, J.V., Ptacek, T.S., Wang, Y., Li, B., Simon, J.M., and Strahl, B.D. (2020). Unique and Shared Roles for Histone H3K36 Methylation States in Transcription Regulation Functions. Cell Reports *31*. 10.1016/j.celrep.2020.107751.
12. Mei, Y.-C., Feng, J., He, F., Li, Y.-M., Liu, Y., Li, F., Chen, Y., and Du, H.-N. (2021). Set2-mediated H3K36 methylation states redundantly repress the production of antisense transcripts: role in transcription regulation. FEBS Open Bio *11*, 2225–2235. https://doi.org/10.1002/2211-5463.13226.
13. Xu, C., Cui, G., Botuyan, M.V., and Mer, G. (2008). Structural basis for the recognition of methylated histone H3K36 by the Eaf3 subunit of histone deacetylase complex Rpd3S. Structure *16*, 1740–1750. 10.1016/j.str.2008.08.008.
14. Leung, C.S., Douglass, S.M., Morselli, M., Obusan, M.B., Pavlyukov, M.S., Pellegrini, M., and Johnson, T.L. (2019). H3K36 Methylation and the

Chromodomain Protein Eaf3 Are Required for Proper Cotranscriptional Spliceosome Assembly. Cell Reports *27*, 3760–3769.e3764. 10.1016/j.celrep.2019.05.100.
15. Guan, H., Wang, P., Zhang, P., Ruan, C., Ou, Y., Peng, B., Zheng, X., Lei, J., Li, B., Yan, C., and Li, H. (2023). Diverse modes of H3K36me3-guided nucleosomal deacetylation by Rpd3S. Nature *620*, 669–675. 10.1038/s41586-023-06349-1.
16. Kim, S., Kim, H., Fong, N., Erickson, B., and Bentley, D.L. (2011). Pre-mRNA splicing is a determinant of histone H3K36 methylation. Proceedings of the National Academy of Sciences *108*, 13564–13569. doi:10.1073/pnas.1109475108.
17. de Almeida, S.F., Grosso, A.R., Koch, F., Fenouil, R., Carvalho, S., Andrade, J., Levezinho, H., Gut, M., Eick, D., Gut, I., et al. (2011). Splicing enhances recruitment of methyltransferase HYPB/Setd2 and methylation of histone H3 Lys36. Nature Structural & Molecular Biology *18*, 977–983. 10.1038/nsmb.2123.
18. Brès, V., Gomes, N., Pickle, L., and Jones, K.A. (2005). A human splicing factor, SKIP, associates with P-TEFb and enhances transcription elongation by HIV-1 Tat. Genes Dev *19*, 1211–1226. 10.1101/gad.1291705.
19. Cao, Y., and Ma, L. (2019). To Splice or to Transcribe: SKIP-Mediated Environmental Fitness and Development in Plants. Front Plant Sci *10*, 1222. 10.3389/fpls.2019.01222.
20. Li, Y., Xia, C., Feng, J., Yang, D., Wu, F., Cao, Y., Li, L., and Ma, L. (2016). The SNW Domain of SKIP Is Required for Its Integration into the Spliceosome and Its Interaction with the Paf1 Complex in Arabidopsis. Molecular Plant *9*, 1040–1050. https://doi.org/10.1016/j.molp.2016.04.011.
21. Abrhámová, K., Groušlová, M., Valentová, A., Hao, X., Liu, B., Převorovský, M., Gahura, O., Půta, F., Sunnerhagen, P., and Folk, P. (2024). Truncating the spliceosomal 'rope protein' Prp45 results in Htz1 dependent phenotypes. RNA Biol *21*, 1–17. 10.1080/15476286.2024.2348896.
22. Wood, A., Krogan, N.J., Dover, J., Schneider, J., Heidt, J., Boateng, M.A., Dean, K., Golshani, A., Zhang, Y., Greenblatt, J.F., et al. (2003). Bre1, an E3 Ubiquitin Ligase Required for Recruitment and Substrate Selection of Rad6 at a Promoter. Molecular Cell *11*, 267–274. 10.1016/S1097-2765(02)00802-X.
23. Vlaming, H., Molenaar, T.M., van Welsem, T., Poramba-Liyanage, D.W., Smith, D.E., Velds, A., Hoekman, L., Korthout, T., Hendriks, S., Altelaar, A.F.M., and van Leeuwen, F. (2016). Direct screening for chromatin status on DNA barcodes in yeast delineates the regulome of H3K79 methylation by Dot1. eLife *5*, e18919. 10.7554/eLife.18919.
24. Schulze, J.M., Hentrich, T., Nakanishi, S., Gupta, A., Emberly, E., Shilatifard, A., and Kobor, M.S. (2011). Splitting the task: Ubp8 and Ubp10 deubiquitinate different cellular pools of H2BK123. Genes Dev *25*, 2242–2247. 10.1101/gad.177220.111.
25. Bilokapic, S., and Halic, M. (2019). Nucleosome and ubiquitin position Set2 to methylate H3K36. Nat Commun *10*, 3795. 10.1038/s41467-019-11726-4.
26. Deng, Z., Ai, H., Sun, M., Tong, Z., Du, Y., Qu, Q., Zhang, L., Xu, Z., Tao, S., Shi, Q., et al. (2023). Mechanistic insights into nucleosomal H2B monoubiquitylation mediated by yeast Bre1-Rad6 and its human homolog

RNF20/RNF40-hRAD6A. Mol Cell *83*, 3080–3094.e3014. 10.1016/j.molcel.2023.08.001.
27. Jorgensen, P., Nishikawa, J.L., Breitkreutz, B.-J., and Tyers, M. (2002). Systematic Identification of Pathways That Couple Cell Growth and Division in Yeast. Science *297*, 395–400. doi:10.1126/science.1070850.
28. Gallego, L.D., Schneider, M., Mittal, C., Romanauska, A., Gudino Carrillo, R.M., Schubert, T., Pugh, B.F., and Köhler, A. (2020). Phase separation directs ubiquitination of gene-body nucleosomes. Nature *579*, 592–597. 10.1038/s41586-020-2097-z.
29. Erdős, G., and Dosztányi, Z. (2024). AIUPred: combining energy estimation with deep learning for the enhanced prediction of protein disorder. Nucleic Acids Research *52*, W176–W181. 10.1093/nar/gkae385.
30. Xiao, T., Kao, C.F., Krogan, N.J., Sun, Z.W., Greenblatt, J.F., Osley, M.A., and Strahl, B.D. (2005). Histone H2B ubiquitylation is associated with elongating RNA polymerase II. Mol Cell Biol *25*, 637–651. 10.1128/mcb.25.2.637-651.2005.
31. Zhao, F., Hicks, C.W., and Wolberger, C. (2023). Mechanism of histone H2B monoubiquitination by Bre1. Nature Structural & Molecular Biology *30*, 1623–1627. 10.1038/s41594-023-01137-x.
32. Song, Y.-H., and Ahn, S.H. (2010). A Bre1-associated Protein, Large 1 (Lge1), Promotes H2B Ubiquitylation during the Early Stages of Transcription Elongation*. Journal of Biological Chemistry *285*, 2361–2367. https://doi.org/10.1074/jbc.M109.039255.
33. Jueun Kim, Y.-K.A., Shinae Park, Jung-Shin Lee (2018). Bre1 mediates the ubiquitination of histone H2B by regulating Lge1 stability. FEBS letters.
34. Daniel, J.A., Torok, M.S., Sun, Z.-W., Schieltz, D., Allis, C.D., Yates, J.R., and Grant, P.A. (2004). Deubiquitination of Histone H2B by a Yeast Acetyltransferase Complex Regulates Transcription*. Journal of Biological Chemistry *279*, 1867–1871. https://doi.org/10.1074/jbc.C300494200.
35. Samara, N.L., Datta, A.B., Berndsen, C.E., Zhang, X., Yao, T., Cohen, R.E., and Wolberger, C. (2010). Structural Insights into the Assembly and Function of the SAGA Deubiquitinating Module. Science *328*, 1025–1029. doi:10.1126/science.1190049.
36. Köhler, A., Zimmerman, E., Schneider, M., Hurt, E., and Zheng, N. (2010). Structural basis for assembly and activation of the heterotetrameric SAGA histone H2B deubiquitinase module. Cell *141*, 606–617. 10.1016/j.cell.2010.04.026.
37. McCormick, M.A., Mason, A.G., Guyenet, S.J., Dang, W., Garza, R.M., Ting, M.K., Moller, R.M., Berger, S.L., Kaeberlein, M., Pillus, L., et al. (2014). The SAGA histone deubiquitinase module controls yeast replicative lifespan via Sir2 interaction. Cell Rep *8*, 477–486. 10.1016/j.celrep.2014.06.037.
38. van der Lee, R., Lang, B., Kruse, K., Gsponer, J., Sánchez de Groot, N., Huynen, M.A., Matouschek, A., Fuxreiter, M., and Babu, M.M. (2014). Intrinsically disordered segments affect protein half-life in the cell and during evolution. Cell Rep *8*, 1832–1844. 10.1016/j.celrep.2014.07.055.

39. Fishbain, S., Inobe, T., Israeli, E., Chavali, S., Yu, H., Kago, G., Babu, M.M., and Matouschek, A. (2015). Sequence composition of disordered regions fine-tunes protein half-life. Nat Struct Mol Biol *22*, 214–221. 10.1038/nsmb.2958.
40. Holehouse, A.S., and Kragelund, B.B. (2024). The molecular basis for cellular function of intrinsically disordered protein regions. Nature Reviews Molecular Cell Biology *25*, 187–211. 10.1038/s41580-023-00673-0.
41. Moses, D., Ginell, G.M., Holehouse, A.S., and Sukenik, S. (2023). Intrinsically disordered regions are poised to act as sensors of cellular chemistry. Trends in Biochemical Sciences *48*, 1019–1034. 10.1016/j.tibs.2023.08.001.
42. Wright, P.E., and Dyson, H.J. (2015). Intrinsically disordered proteins in cellular signalling and regulation. Nature Reviews Molecular Cell Biology *16*, 18–29. 10.1038/nrm3920.
43. van der Horst, S.C., Kollenstart, L., Batté, A., Keizer, S., Vreeken, K., Pandey, P., Chabes, A., and van Attikum, H. (2025). Replication-IDentifier links epigenetic and metabolic pathways to the replication stress response. Nature Communications *16*, 1416. 10.1038/s41467-025-56561-y.
44. Shi, M., Wang, X., Zhang, H., Wen, Y., Liu, Q., Chen, P., Chen, X., and Xiang, S. (2026). Structural insights into the Bre1–Lge1 and RNF20/RNF40–WAC interactions critical for H2B ubiquitination. Nucleic Acids Research *54*. 10.1093/nar/gkaf1514.
45. Larochelle, M., Bergeron, D., Arcand, B., and Bachand, F. (2019). Proximity-dependent biotinylation mediated by TurboID to identify protein-protein interaction networks in yeast. J Cell Sci *132*. 10.1242/jcs.232249.
46. Mirdita, M., Schütze, K., Moriwaki, Y., Heo, L., Ovchinnikov, S., and Steinegger, M. (2022). ColabFold: making protein folding accessible to all. Nature Methods *19*, 679–682. 10.1038/s41592-022-01488-1.
47. Stringer, C., Wang, T., Michaelos, M., and Pachitariu, M. (2021). Cellpose: a generalist algorithm for cellular segmentation. Nature Methods *18*, 100–106. 10.1038/s41592-020-01018-x.
48. Hwang, W.W., Venkatasubrahmanyam, S., Ianculescu, A.G., Tong, A., Boone, C., and Madhani, H.D. (2003). A Conserved RING Finger Protein Required for Histone H2B Monoubiquitination and Cell Size Control. Molecular Cell *11*, 261–266. https://doi.org/10.1016/S1097-2765(02)00826-2.
49. Ambrozková, M., Půta, F., Fuková, I., Skružný, M., Brábek, J., and Folk, P. (2001). The Fission Yeast Ortholog of the Coregulator SKIP Interacts with the Small Subunit of U2AF. Biochemical and Biophysical Research Communications *284*, 1148–1154. https://doi.org/10.1006/bbrc.2001.5108.
50. Cao, Y., Wen, L., Wang, Z., and Ma, L. (2015). SKIP Interacts with the Paf1 Complex to Regulate Flowering via the Activation of FLC Transcription in Arabidopsis. Molecular Plant *8*, 1816–1819. 10.1016/j.molp.2015.09.004.
51. Farag, M., Cohen, S.R., Borcherds, W.M., Bremer, A., Mittag, T., and Pappu, R.V. (2022). Condensates formed by prion-like low-complexity domains have small-world network structures and interfaces defined by expanded conformations. Nature Communications *13*, 7722. 10.1038/s41467-022-35370-7.

52. Villegas, J.A., Heidenreich, M., and Levy, E.D. (2022). Molecular and environmental determinants of biomolecular condensate formation. Nature Chemical Biology *18*, 1319–1329. 10.1038/s41589-022-01175-4.
53. Pei, G., Lyons, H., Li, P., and Sabari, B.R. (2025). Transcription regulation by biomolecular condensates. Nature Reviews Molecular Cell Biology *26*, 213–236. 10.1038/s41580-024-00789-x.
54. Wang, Y., Li, S., Mokbel, M., May, A.I., Liang, Z., Zeng, Y., Wang, W., Zhang, H., Yu, F., Sporbeck, K., et al. (2024). Biomolecular condensates mediate bending and scission of endosome membranes. Nature *634*, 1204–1210. 10.1038/s41586-024-07990-0.
55. Dai, Y., Zhou, Z., Yu, W., Ma, Y., Kim, K., Rivera, N., Mohammed, J., Lantelme, E., Hsu-Kim, H., Chilkoti, A., and You, L. (2024). Biomolecular condensates regulate cellular electrochemical equilibria. Cell *187*, 5951–5966.e5918. 10.1016/j.cell.2024.08.018.
56. Zhang, F., and Yu, X. (2011). WAC, a functional partner of RNF20/40, regulates histone H2B ubiquitination and gene transcription. Mol Cell *41*, 384–397. 10.1016/j.molcel.2011.01.024.
57. Liu, Y., Koornneef, M., and Soppe, W.J. (2007). The absence of histone H2B monoubiquitination in the Arabidopsis hub1 (rdo4) mutant reveals a role for chromatin remodeling in seed dormancy. Plant Cell *19*, 433–444. 10.1105/tpc.106.049221.
58. Hérissant, L., Moehle, E.A., Bertaccini, D., Van Dorsselaer, A., Schaeffer-Reiss, C., Guthrie, C., and Dargemont, C. (2014). H2B ubiquitylation modulates spliceosome assembly and function in budding yeast. Biol Cell *106*, 126–138. 10.1111/boc.201400003.
59. Shieh, G.S., Pan, C.H., Wu, J.H., Sun, Y.J., Wang, C.C., Hsiao, W.C., Lin, C.Y., Tung, L., Chang, T.H., Fleming, A.B., et al. (2011). H2B ubiquitylation is part of chromatin architecture that marks exon-intron structure in budding yeast. BMC Genomics *12*, 627. 10.1186/1471-2164-12-627.
60. Jung, I., Kim, S.K., Kim, M., Han, Y.M., Kim, Y.S., Kim, D., and Lee, D. (2012). H2B monoubiquitylation is a 5'-enriched active transcription mark and correlates with exon-intron structure in human cells. Genome Res *22*, 1026–1035. 10.1101/gr.120634.111.
61. Krogan, N.J., Kim, M., Tong, A., Golshani, A., Cagney, G., Canadien, V., Richards, D.P., Beattie, B.K., Emili, A., Boone, C., et al. (2003). Methylation of histone H3 by Set2 in Saccharomyces cerevisiae is linked to transcriptional elongation by RNA polymerase II. Mol Cell Biol *23*, 4207–4218. 10.1128/mcb.23.12.4207-4218.2003.
62. Costanzo, M., VanderSluis, B., Koch, E.N., Baryshnikova, A., Pons, C., Tan, G., Wang, W., Usaj, M., Hanchard, J., Lee, S.D., et al. (2016). A global genetic interaction network maps a wiring diagram of cellular function. Science *353*. 10.1126/science.aaf1420.
63. Tong, A.H., Lesage, G., Bader, G.D., Ding, H., Xu, H., Xin, X., Young, J., Berriz, G.F., Brost, R.L., Chang, M., et al. (2004). Global mapping of the yeast genetic interaction network. Science *303*, 808–813. 10.1126/science.1091317.

64. Krogan, N.J., Baetz, K., Keogh, M.C., Datta, N., Sawa, C., Kwok, T.C., Thompson, N.J., Davey, M.G., Pootoolal, J., Hughes, T.R., et al. (2004). Regulation of chromosome stability by the histone H2A variant Htz1, the Swr1 chromatin remodeling complex, and the histone acetyltransferase NuA4. Proc Natl Acad Sci U S A *101*, 13513–13518. 10.1073/pnas.0405753101.
65. Venkatasubrahmanyam, S., Hwang, W.W., Meneghini, M.D., Tong, A.H., and Madhani, H.D. (2007). Genome-wide, as opposed to local, antisilencing is mediated redundantly by the euchromatic factors Set1 and H2A.Z. Proc Natl Acad Sci U S A *104*, 16609–16614. 10.1073/pnas.0700914104.
66. Bähler, J., Wu, J.Q., Longtine, M.S., Shah, N.G., McKenzie, A., 3rd, Steever, A.B., Wach, A., Philippsen, P., and Pringle, J.R. (1998). Heterologous modules for efficient and versatile PCR-based gene targeting in Schizosaccharomyces pombe. Yeast *14*, 943–951. 10.1002/(sici)1097-0061(199807)14:10<943::Aid-yea292>3.0.Co;2-y.
67. Lemay, J.-F., Marguerat, S., Larochelle, M., Liu, X., van Nues, R., Hunyadkürti, J., Hoque, M., Tian, B., Granneman, S., and Bähler, J. (2016). The Nrd1-like protein Seb1 coordinates cotranscriptional 3′ end processing and polyadenylation site selection. Genes & development *30*, 1558–1572.

Figure 1

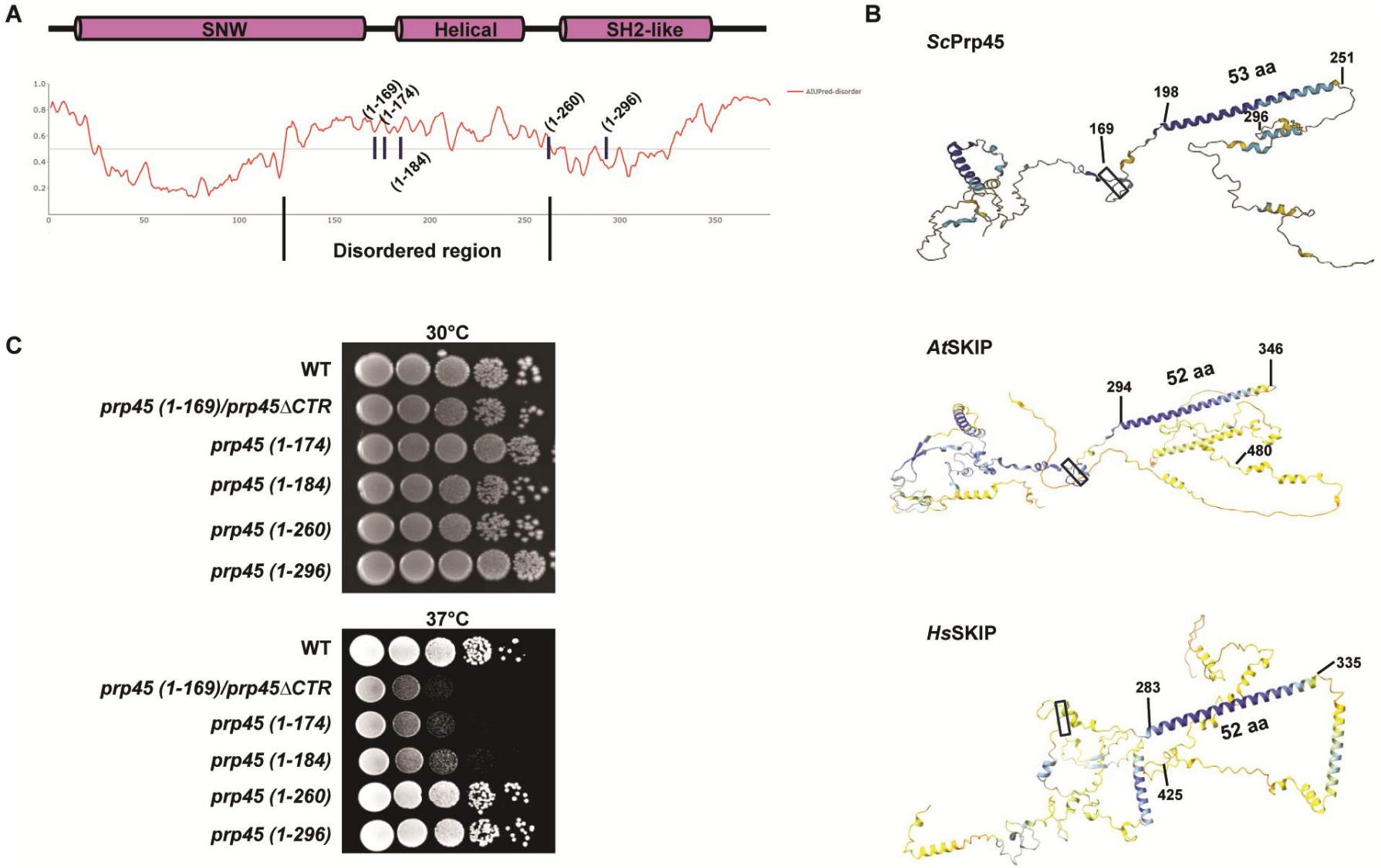
A
SNW
Helical
SH2-like
AIUPred-disorder
(1-169)
(1-174)
(1-184)
(1-260)
(1-296)
Disordered region
B
ScPrp45
53 aa
251
198
169
296
AtSKIP
52 aa
346
294
480
HsSKIP
52 aa
335
283
425
C
30°C
WT
prp45 (1-169)/prp45ΔCTR
prp45 (1-174)
prp45 (1-184)
prp45 (1-260)
prp45 (1-296)
37°C
WT
prp45 (1-169)/prp45ΔCTR
prp45 (1-174)
prp45 (1-184)
prp45 (1-260)
prp45 (1-296)

Figure 2

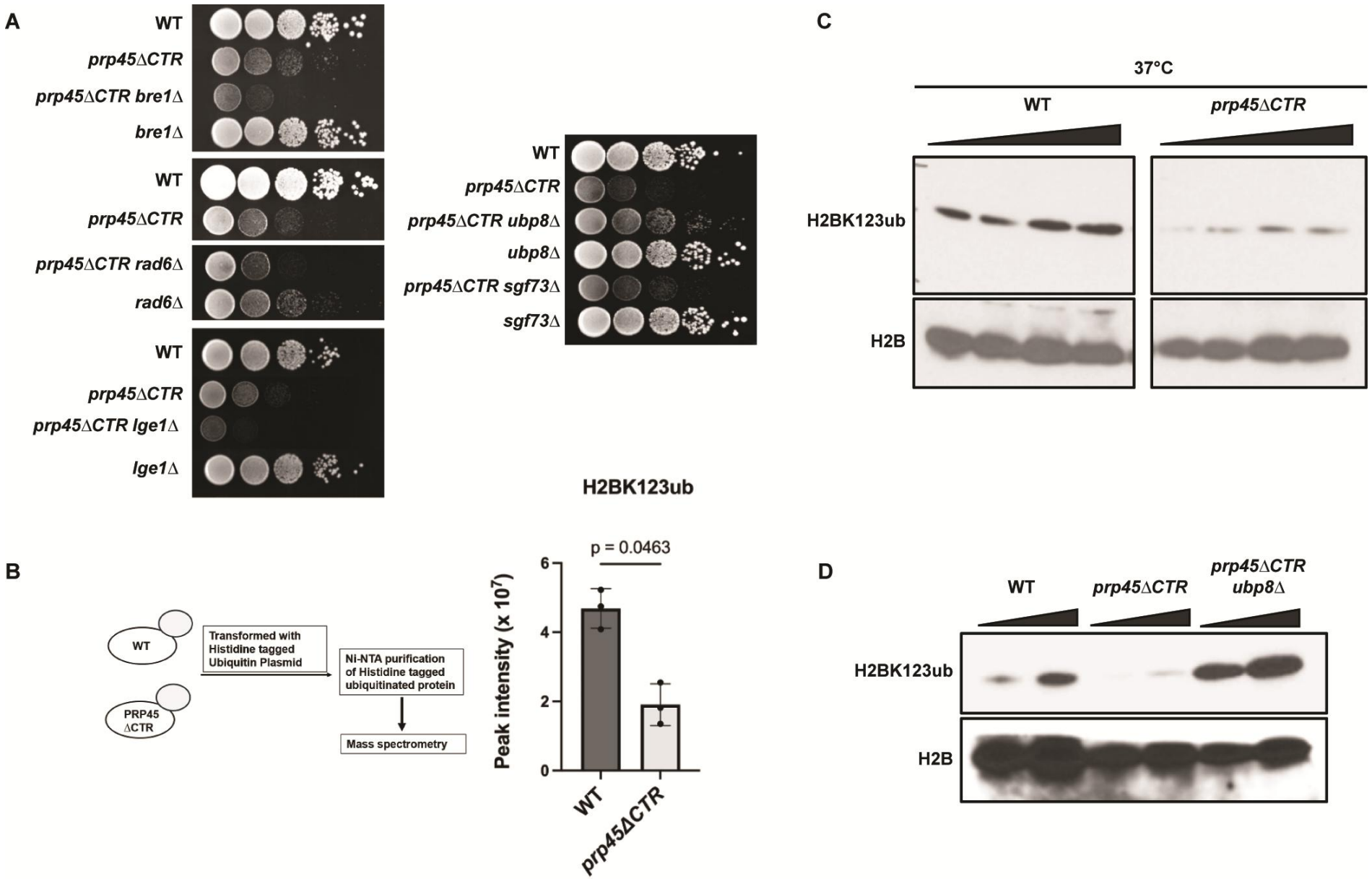
A
WT
prp45ΔCTR
prp45ΔCTR bre1Δ
bre1Δ
WT
prp45ΔCTR
prp45ΔCTR rad6Δ
rad6Δ
WT
prp45ΔCTR
prp45ΔCTR lge1Δ
lge1Δ
WT
prp45ΔCTR
prp45ΔCTR ubp8Δ
ubp8Δ
prp45ΔCTR sgf73Δ
sgf73Δ
C
37°C
WT
prp45ΔCTR
H2BK123ub
H2B
B
WT
PRP45 ΔCTR
Transformed with Histidine tagged Ubiquitin Plasmid
Ni-NTA purification of Histidine tagged ubiquitinated protein
Mass spectrometry
H2BK123ub
p = 0.0463
Peak intensity (x 10^7)
6
4
2
0
WT
prp45ΔCTR
D
WT
prp45ΔCTR
prp45ΔCTR ubp8Δ
H2BK123ub
H2B

Figure 3

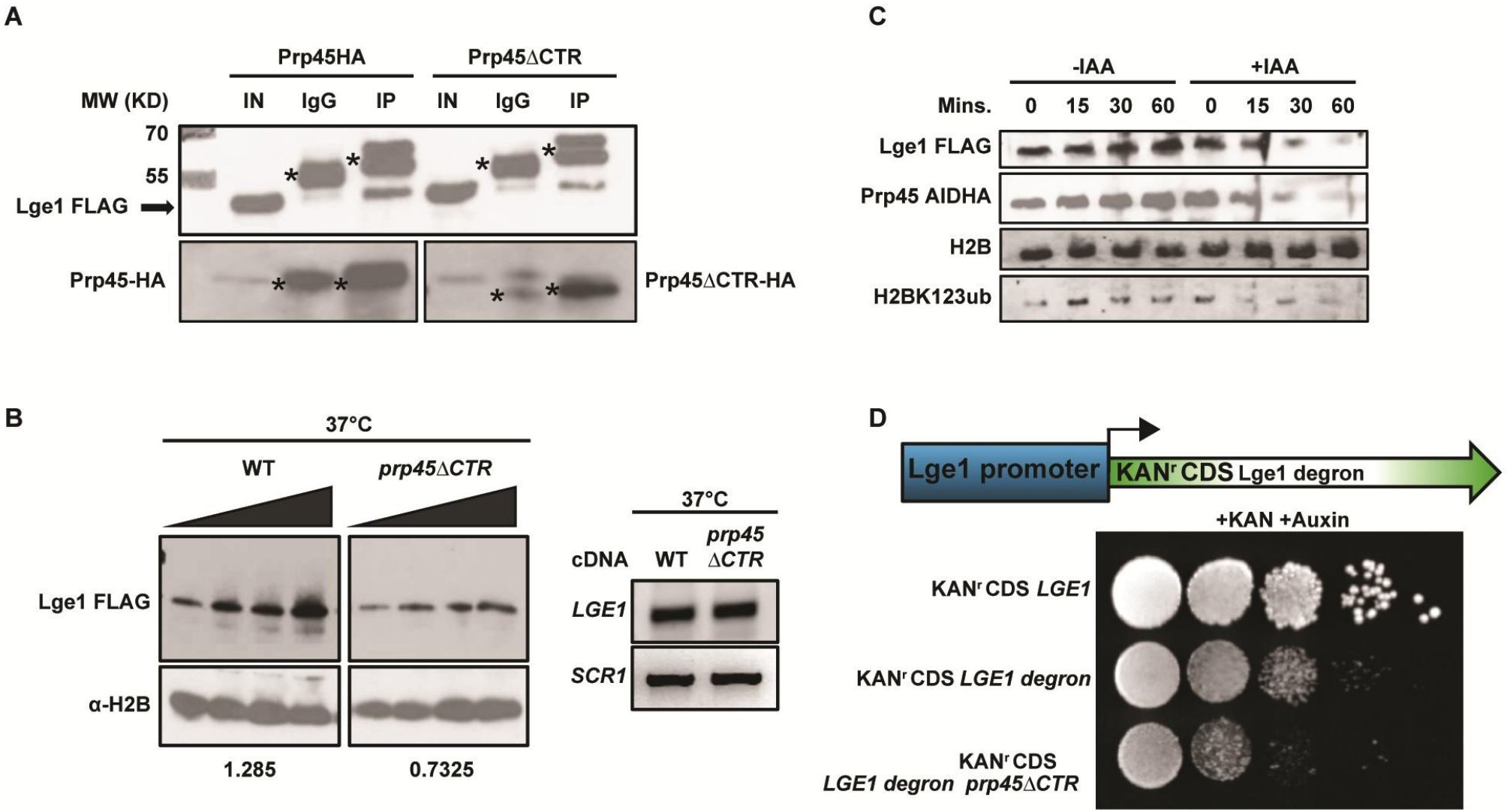
A
Prp45HA
Prp45ΔCTR
MW (KD)
IN
IgG
IP
IN
IgG
IP
70
55
Lge1 FLAG
Prp45-HA
Prp45ΔCTR-HA
B
37°C
WT
prp45ΔCTR
Lge1 FLAG
α-H2B
1.285
0.7325
37°C
cDNA
WT
prp45 ΔCTR
LGE1
SCR1
C
-IAA
+IAA
Mins.
0
15
30
60
0
15
30
60
Lge1 FLAG
Prp45 AIDHA
H2B
H2BK123ub
D
Lge1 promoter
KANr CDS Lge1 degron
+KAN +Auxin
KANr CDS LGE1
KANr CDS LGE1 degron
KANr CDS
LGE1 degron prp45ΔCTR

Figure 4

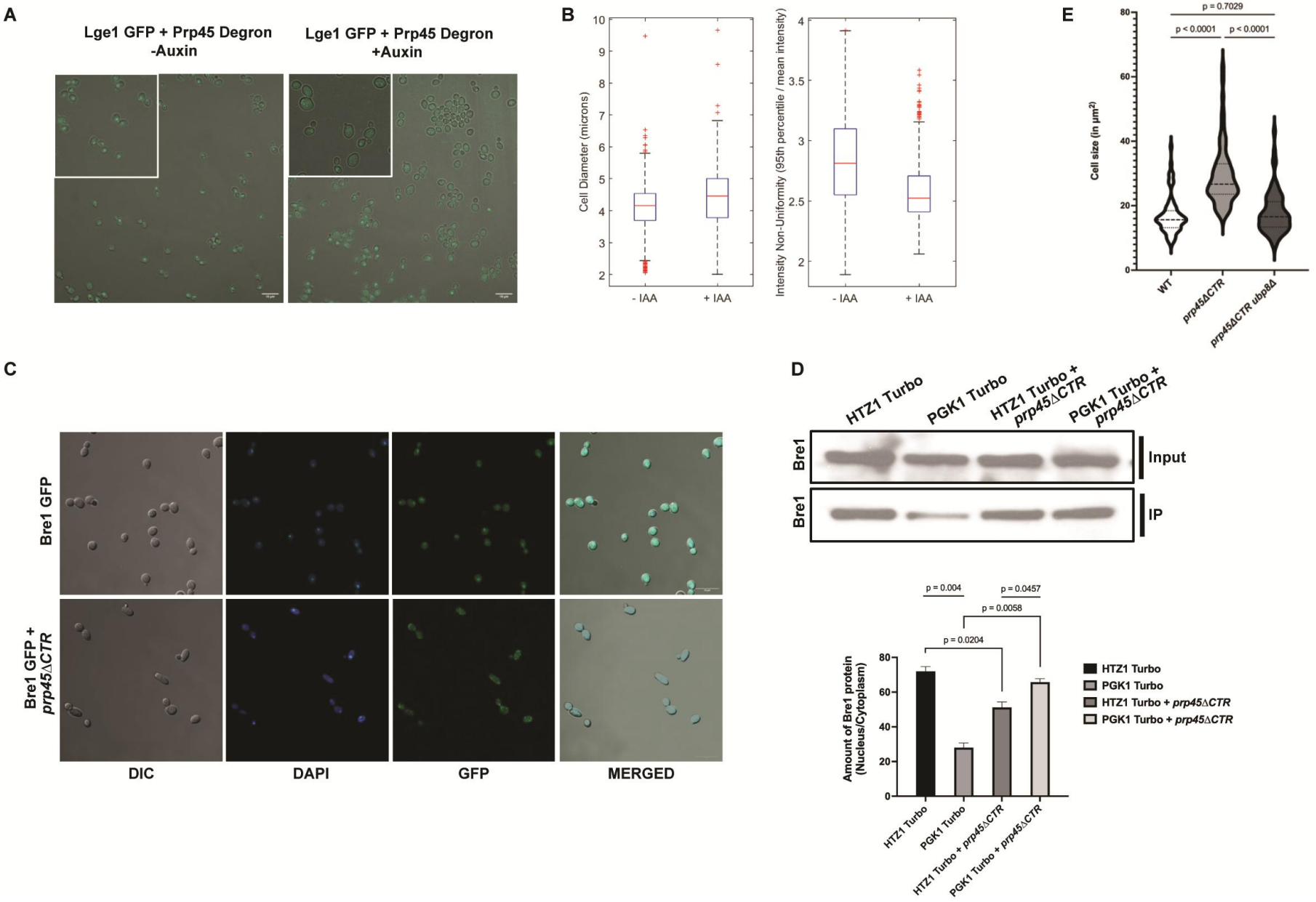
A
Lge1 GFP + Prp45 Degron -Auxin
Lge1 GFP + Prp45 Degron +Auxin
B
Cell Diameter (microns)
- IAA
+ IAA
Intensity Non-Uniformity (95th percentile / mean intensity)
- IAA
+ IAA
E
p = 0.7029
p < 0.0001
p < 0.0001
Cell size (in µm²)
WT
prp45ΔCTR
prp45ΔCTR ubp8Δ
C
Bre1 GFP
Bre1 GFP + prp45ΔCTR
DIC
DAPI
GFP
MERGED
D
HTZ1 Turbo
PGK1 Turbo
HTZ1 Turbo + prp45ΔCTR
PGK1 Turbo + prp45ΔCTR
Bre1
Input
Bre1
IP
p = 0.004
p = 0.0457
p = 0.0058
p = 0.0204
Amount of Bre1 protein (Nucleus/Cytoplasm)
HTZ1 Turbo
PGK1 Turbo
HTZ1 Turbo + prp45ΔCTR
PGK1 Turbo + prp45ΔCTR

Figure 5

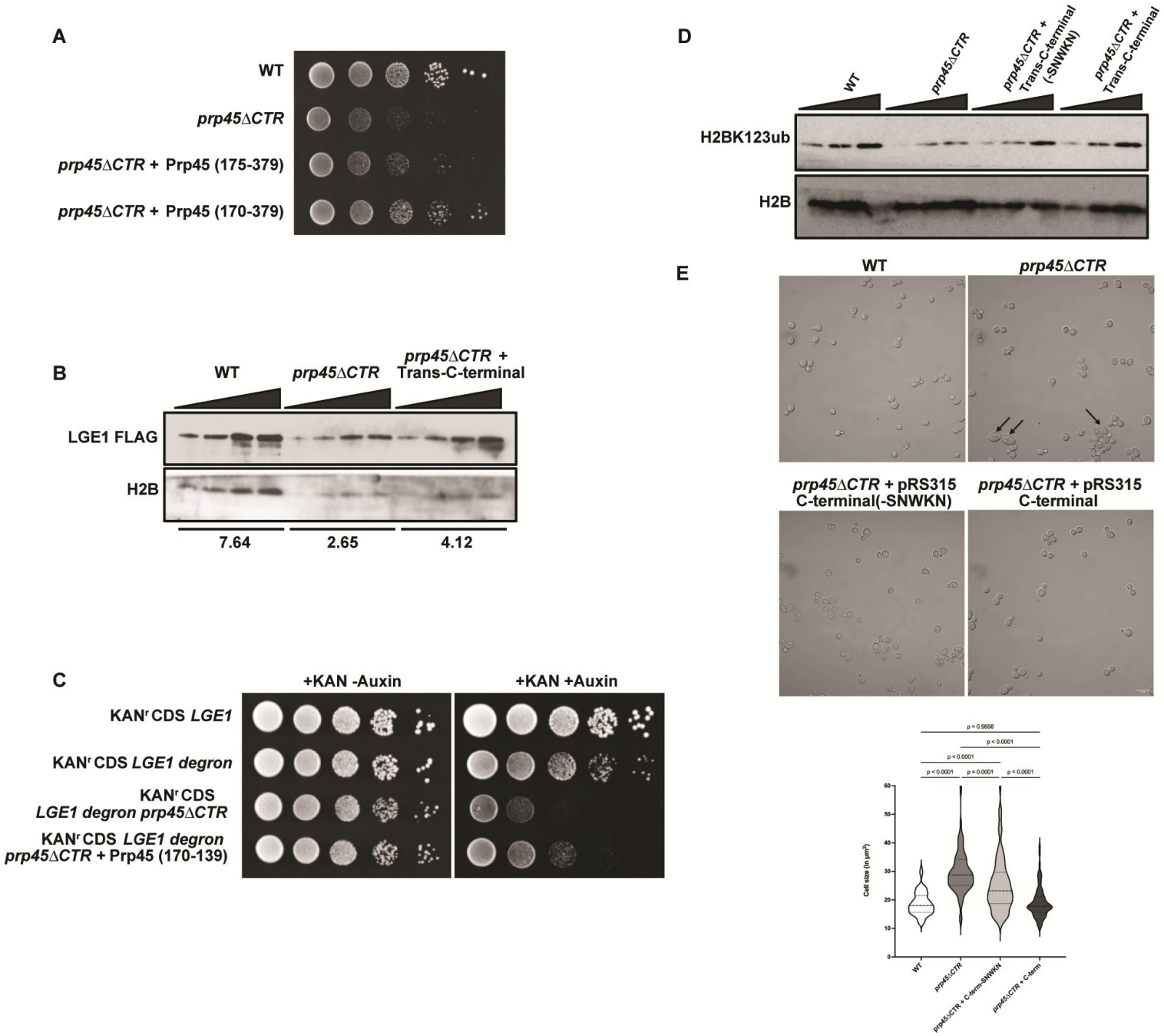
A
WT
prp45ΔCTR
prp45ΔCTR + Prp45 (175-379)
prp45ΔCTR + Prp45 (170-379)
B
WT
prp45ΔCTR
prp45ΔCTR + Trans-C-terminal
LGE1 FLAG
H2B
7.64
2.65
4.12
C
+KAN -Auxin
+KAN +Auxin
KANr CDS LGE1
KANr CDS LGE1 degron
KANr CDS LGE1 degron prp45ΔCTR
KANr CDS LGE1 degron prp45ΔCTR + Prp45 (170-139)
D
WT
prp45ΔCTR
prp45ΔCTR + Trans-C-terminal (-SNWKN)
prp45ΔCTR + Trans-C-terminal
H2BK123ub
H2B
E
WT
prp45ΔCTR
prp45ΔCTR + pRS315 C-terminal(-SNWKN)
prp45ΔCTR + pRS315 C-terminal
p = 0.9856
p < 0.0001
p < 0.0001
p < 0.0001
p = 0.0001
p < 0.0001
Cell size (in μm²)
WT
prp45ΔCTR
prp45ΔCTR + C-term-SNWKN
prp45ΔCTR + C-term

Figure 6

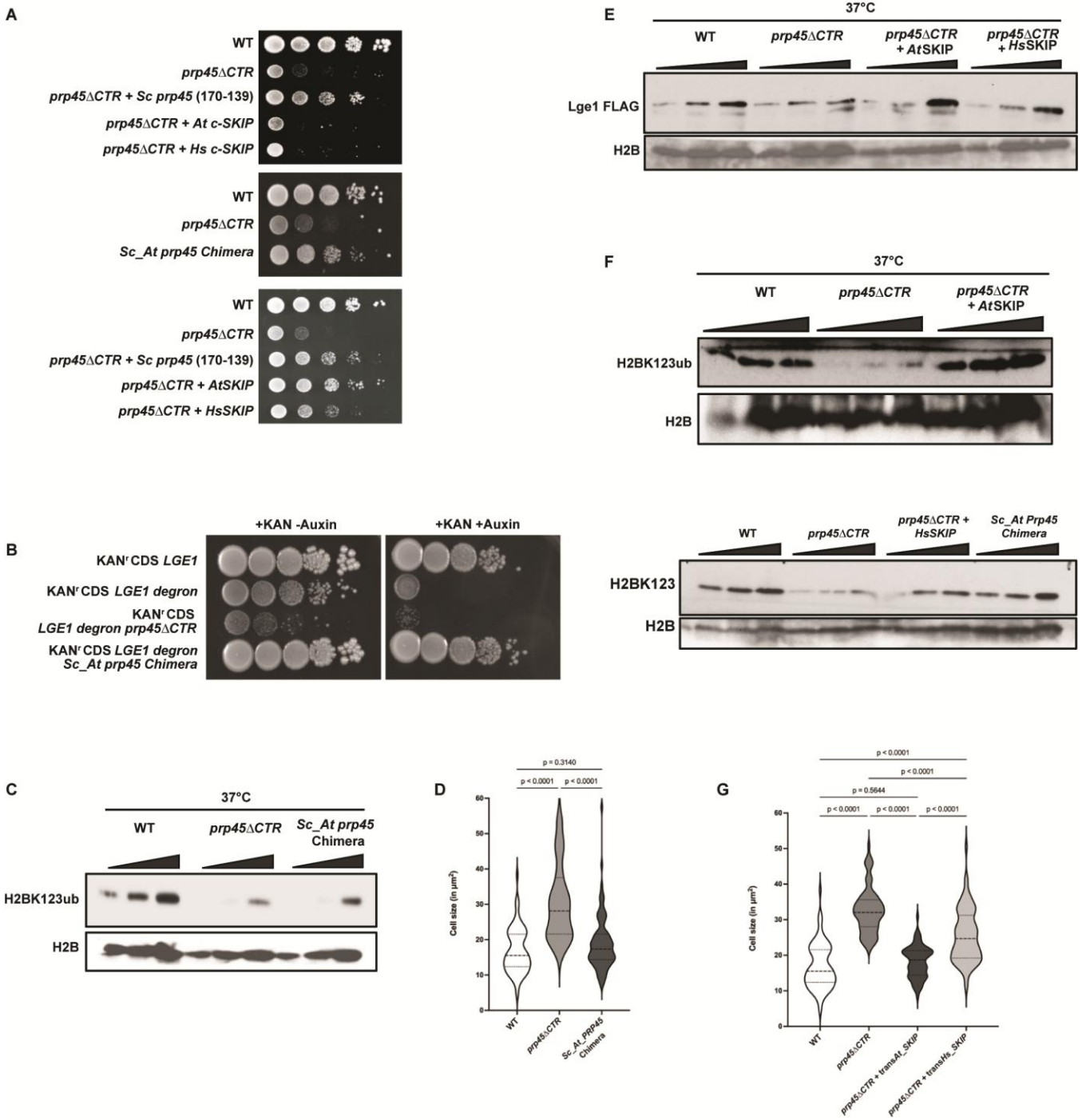
A
WT
prp45ΔCTR
prp45ΔCTR + Sc prp45 (170-139)
prp45ΔCTR + At c-SKIP
prp45ΔCTR + Hs c-SKIP
WT
prp45ΔCTR
Sc_At prp45 Chimera
WT
prp45ΔCTR
prp45ΔCTR + Sc prp45 (170-139)
prp45ΔCTR + AtSKIP
prp45ΔCTR + HsSKIP
B
+KAN -Auxin
+KAN +Auxin
KANr CDS LGE1
KANr CDS LGE1 degron
KANr CDS LGE1 degron prp45ΔCTR
KANr CDS LGE1 degron Sc_At prp45 Chimera
C
37°C
WT
prp45ΔCTR
Sc_At prp45 Chimera
H2BK123ub
H2B
D
p = 0.3140
p < 0.0001
p < 0.0001
Cell size (in µm²)
WT
prp45ΔCTR
Sc_At_Prp45 Chimera
E
37°C
WT
prp45ΔCTR
prp45ΔCTR + AtSKIP
prp45ΔCTR + HsSKIP
Lge1 FLAG
H2B
F
37°C
WT
prp45ΔCTR
prp45ΔCTR + AtSKIP
H2BK123ub
H2B
WT
prp45ΔCTR
prp45ΔCTR + HsSKIP
Sc_At Prp45 Chimera
H2BK123
H2B
G
p < 0.0001
p < 0.0001
p = 0.5644
p < 0.0001
p < 0.0001
p < 0.0001
Cell size (in µm²)
WT
prp45ΔCTR
prp45ΔCTR + transAt_SKIP
prp45ΔCTR + transHs_SKIP

Figure 7

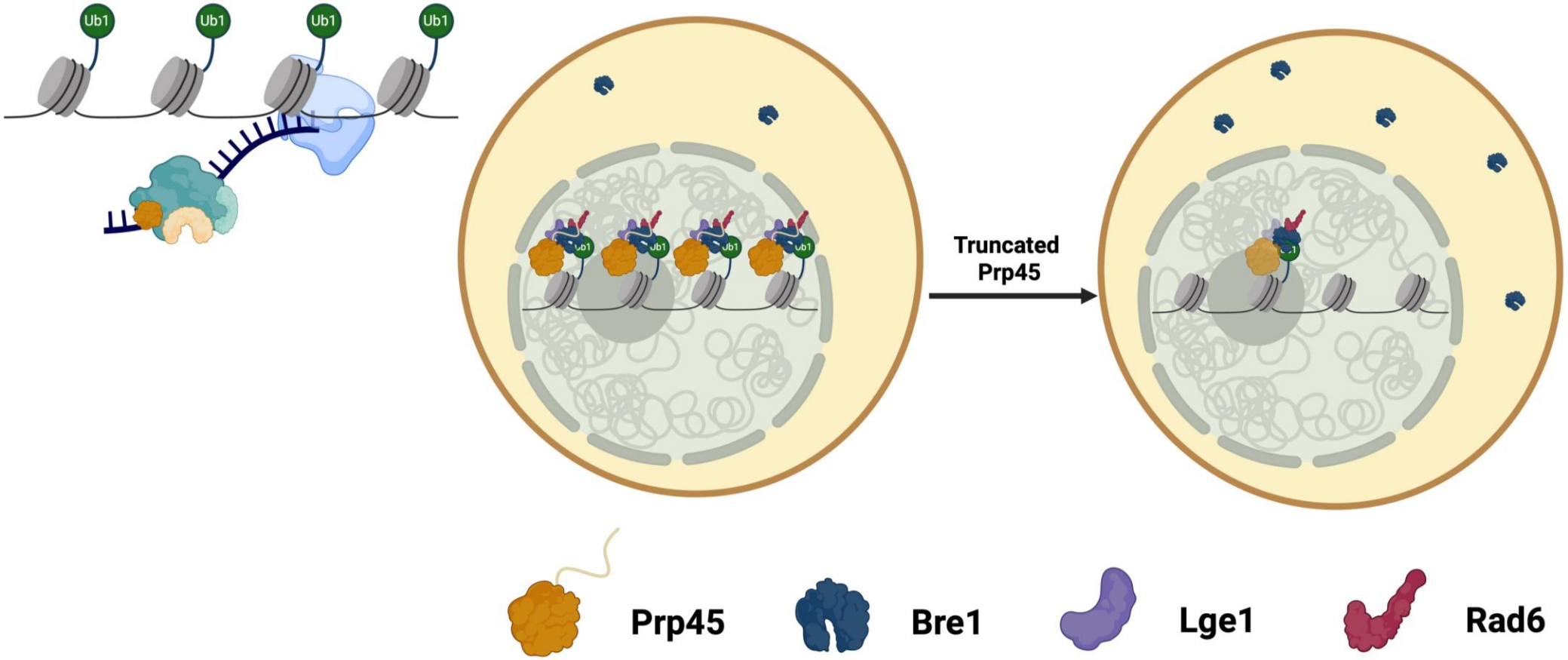

Supplementary figure 1

```
At   MKSLNDLPAPKSTTTTYYDHSNDAWFKNRVTESETVKSSSIKFKVVPAYLNRQGLRPKNP
Hs   MALTSFLPAPTQLSQDQLEAEEKARSQ-RSRQTSLVSSR----REPPPYGYRKGWIPRLL
Sc   -MFSNRLPPPKHS---------------------------------------------
         . **.*.

At   EDFGDGGAFPEIHLPQYPLLMGKNKSNKPGAKTLPVTVDAQGNVVFDAIVRQNENSRKIV
Hs   EDFGDGGAFPEIHVAQYPLDMGRKKK---MSNALAIQVDSEGKIKYDAIARQGQSKDKVI
Sc   -----------------------------------QGRVSTALSSDRVEPAILTDQIAK
                                          .  :  * :     ..

At   YSQHKDIIPKFLKNEGDLGTVVDEEEELQKEIQETAEETKAAIEKIVNVRLSAAQPSNIA
Hs   YSKYTDLVPKEVMNADDP----DLQRPDEEAIKEITEKTRVALEKSVSQKVAAAMPVRAA
Sc   NVKLDDFIPKRQSNFELS-----VPLPTKAEIQECTARTKSYIQRLVNAKLANSNNRASS
       :  *::**   *             :  *:* : .*:  ::: *. ::: :     :

At   RQSGDSQYIKYKPSQQSSAFNSGAKERIIRMVEMPVDPLDPPKFKH-KRVPRASGS--PP
Hs   DKLAPAQYIRYTPSQQGVAFNSGAKQRVIRMVEMQKDPMEPPRFKINKKIPRGPPS--PP
Sc   R--------YVTETHQAPANLLLNNSHHIEVVSKQMDPLLPRFVGKKARKVVAPTENDEV
                  . ::*. *     :.: *.:*.   **: *  .    :   .. .

At   VPVMHSP-PRPVTVKDQQDWKIPPCISNWKNPKGYTIPLDKRLAADGRGLQDVQINDNFA
Hs   APVMHSP-SRKMTVKEQQEWKIPPCISNWKNAKGYTIPLDKRLAADGRGLQTVHINENFA
Sc   VPVLHMDGSNDRGEADPNEWKIPAAVSNWKNPNGYTVALERRVGKALD-NENNTINDGFM
     .**:*   ..     : ::****..:*****.:***:.*::*:.      :   **:.*

At   KLSEALYVAEQKAREAVSMRSKVQKEMVMKDKERKEQELRALAQKARSERTGAAMSMPVS
Hs   KLAEALYIADRKAREAVEMRAQVERKMAQKEKEKHEEKLREMAQKARERRAGIKTHVEKE
Sc   KLSEALENADKKARQEIRSKMELKRLAMEQEMLAKESKLKELSQRARYHNGTPQTGAIVK
     **:***  *::***: :  : ::::    ::   :*.:*: ::*:** ..         .

At   SDRGRSESVDPRGDYDNYDQDRGRERERERERPQETREEREKRIQREKIREERRRERERERR
Hs   DGEAR-----------------------------------ERDEIRHDRRKERQHDR-
Sc   P-------------------------------------------------------

At   LDAKDAAMGKKSKITRDRDRDISEKVALGMASTGGKGGGEVMYDQRLFNQDKGMDSGFAA
Hs   -NLSRAAPDKRSKLQRNENRDISEVIALGVPNP--RTSNEVQYDQRLFNQSKGMDSGFAG
Sc   -KKQTSTVARLKELAYSQGRDVSEKIILGAAKR--SEQPDLQYDSRFFTRG-----ANAS
      . . ::  : .::  ...**:** : ** ..      :: **.*:*.:.     . *.

At   --DDQYNLYDKGLFTAQPTLSTLYKPKKDNDEEMYGNADEQLDKIKNTERFKPDKAFTGA
Hs   GEDEIYNVYDQAWRGGKDMAQSIYRPSKNLDKDMYG---DDLEARIKTNRFVPDKEFSGS
Sc   AKRHEDQVYDNPLFVQQ----------------------DIESIYKTNYEKLDEAVNVK
        .  ::**:     :                       :::   :*:    *: ..

At   SERVGSKRDRPVEFEKEEEQDPFGLEKWVSDLKKGKKPLDKIGSGGTMRASGGGGSSSRD
Hs   DRRQRG-REGPVQFE----EDPFGLDKFLEEAKQH---------GGSKRPSDS--SRPKE
Sc   SEGASG-SHGPIQFT---------------------------------------KAESD
     ..   .  . *::*                                          .   :

At   DDHGGSGRTKINFERSDRR
Hs   HEHEGKKRRKE--------
Sc   DKSDNYGA-----------
     ..  .
```

Highlighted blue box: SNW domain
Highlighted red box: SNW motif
Highlighted green box: Disordered region
Highlighted yellow line: SH2 like domain

Table S1

Pathways	Specific Complex	Proteins
RNA Processing	Spliceosome (Core & NTC)	PRP8, PRP2, SLU7, CWC22, CWC25, CEF1, ISY1, SYF1, SYF2, BUD13, IST3, SNU66, CDC40, ECM2, FDO1
RNA Processing	mRNA Processing/Exosome	HRP1, LRP1
Ribosome Biogenesis	SSU Processome / 90S	KRI1, IMP4, ECM16, RIX1, GCD10
Chromatin & Transcription	Chromatin/Silencing (SIR)	SIR2, SIR4, BRE1
Chromatin & Transcription	Transcription Factors/Stress	REB1, HSF1, MBF1, TOD6, CTK1, SGV1
DNA Metabolism	DNA Replication/Repair	MRC1, RFC5, RNR4
Nuclear/Other	Nuclear Transport/Mod.	NUP1, UBA2
Nuclear/Other	Metabolism/Redox	GRX1, IGD1

Supplementary figure 2

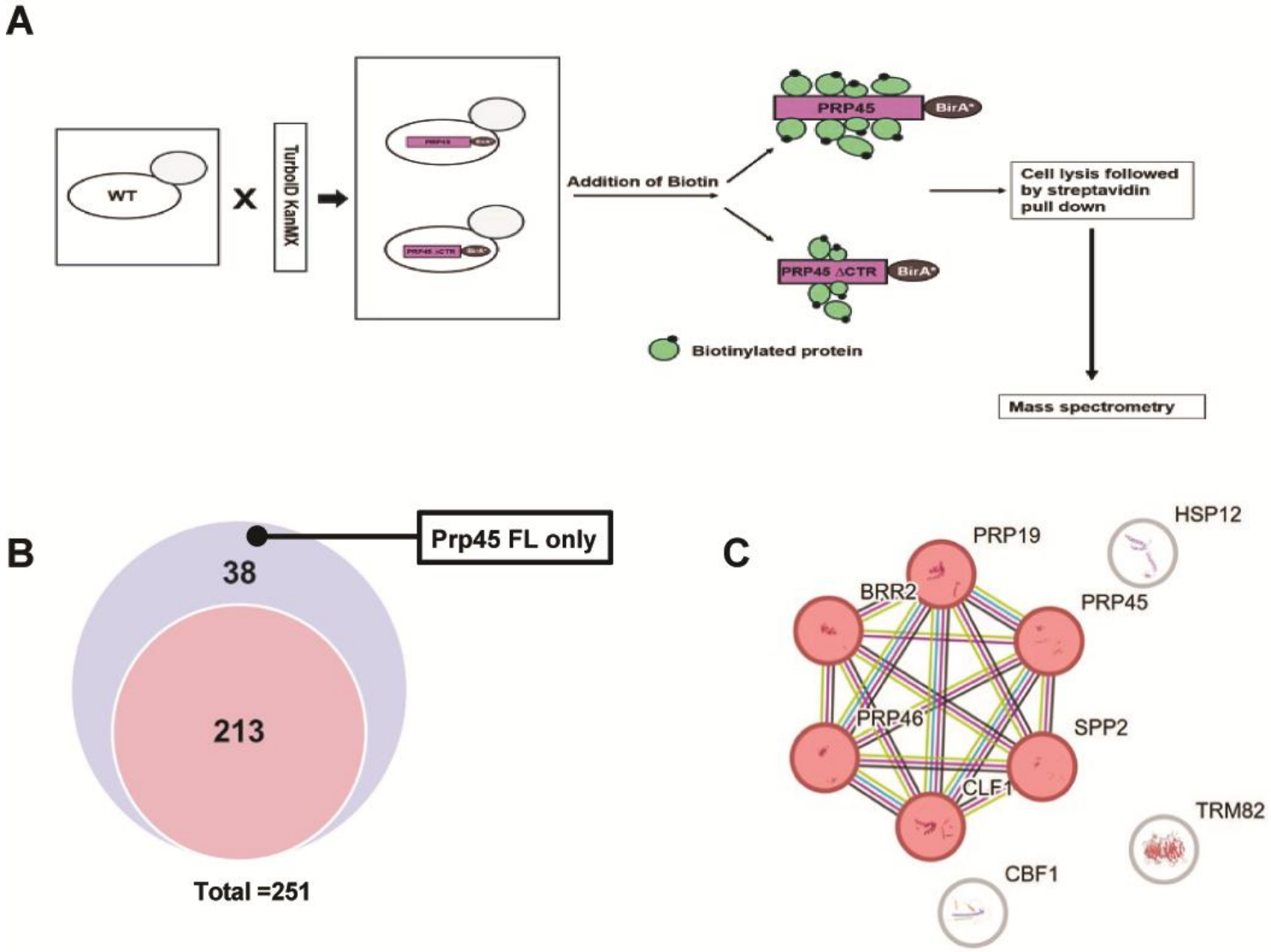

Supplementary figure 3

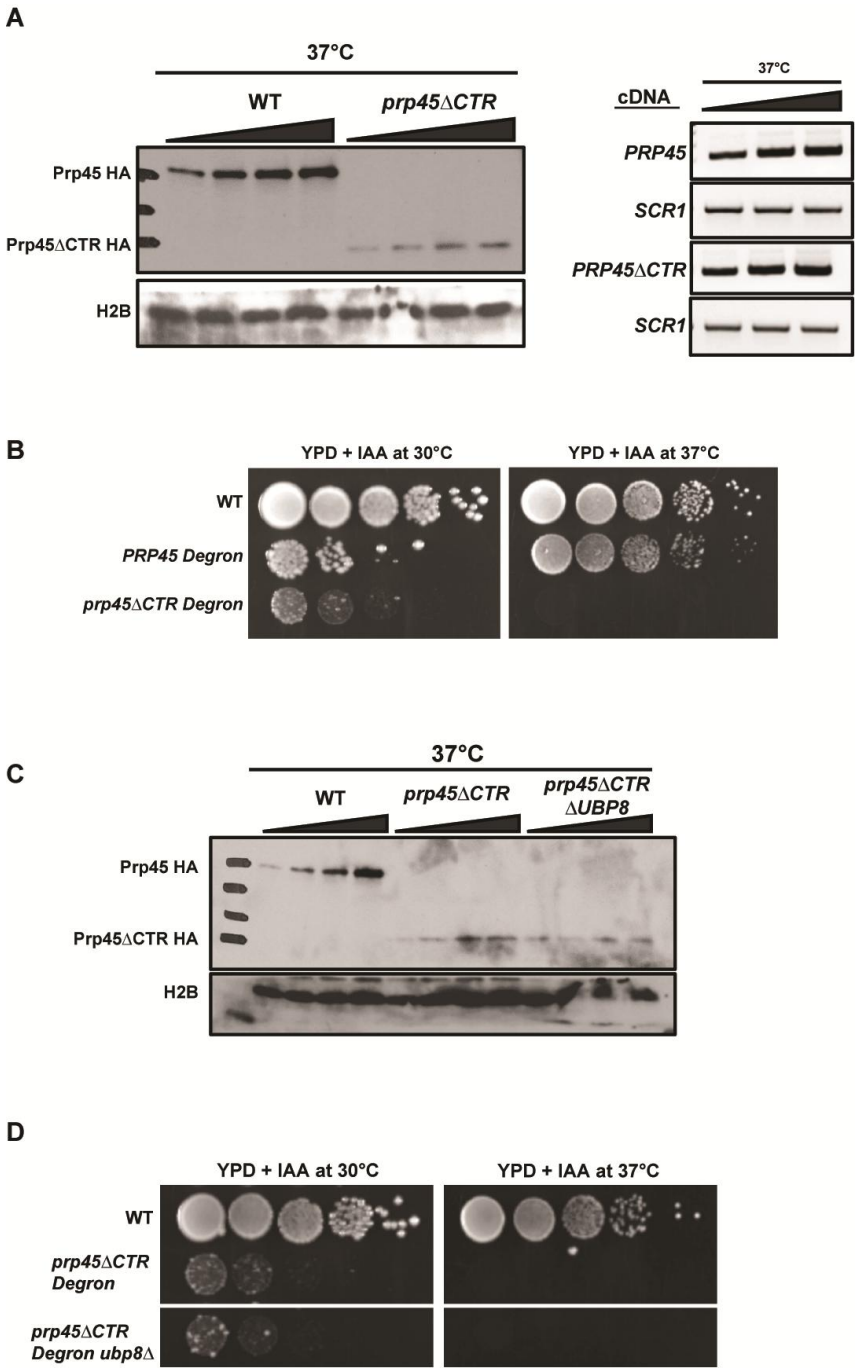

Supplementary figure 4

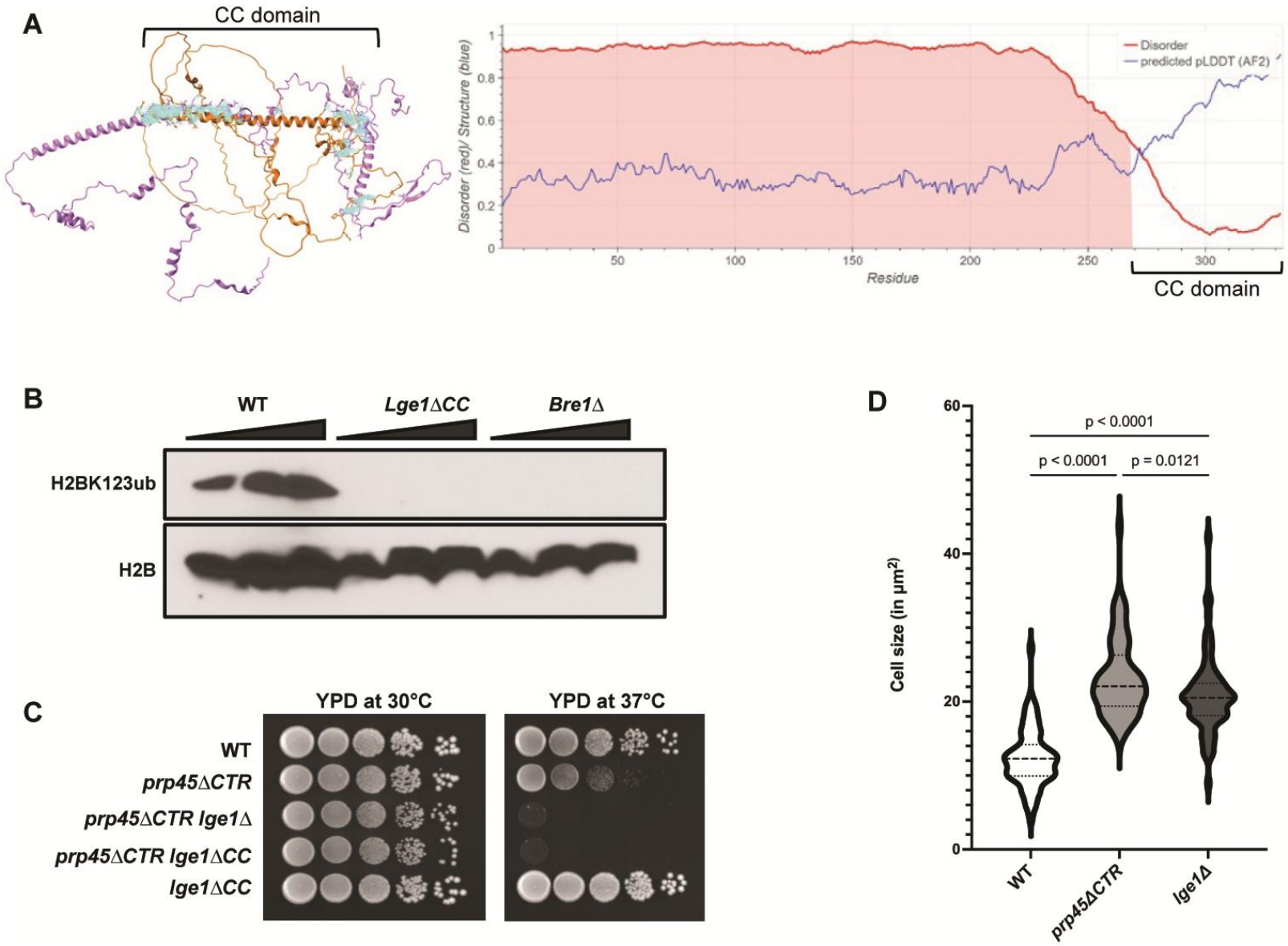

Supplementary figure 5

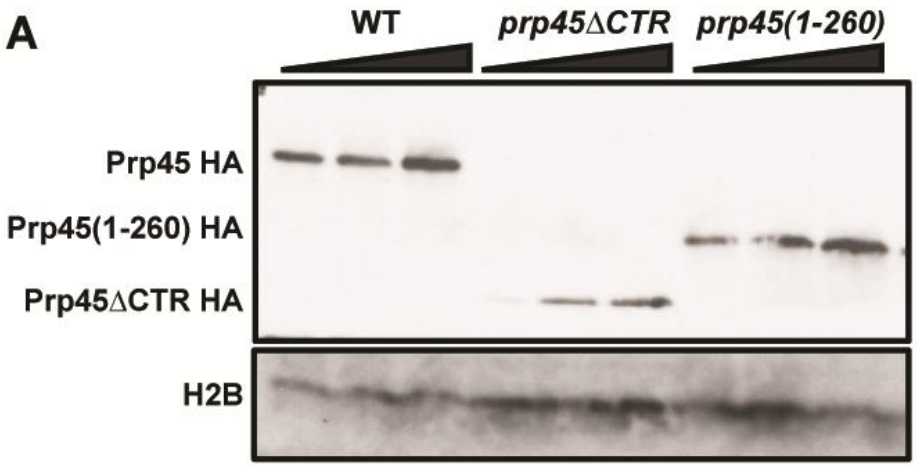

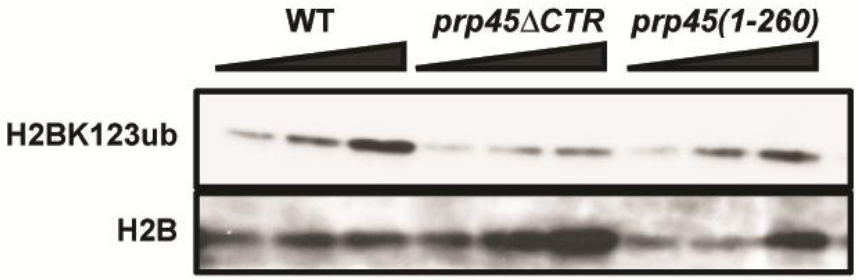

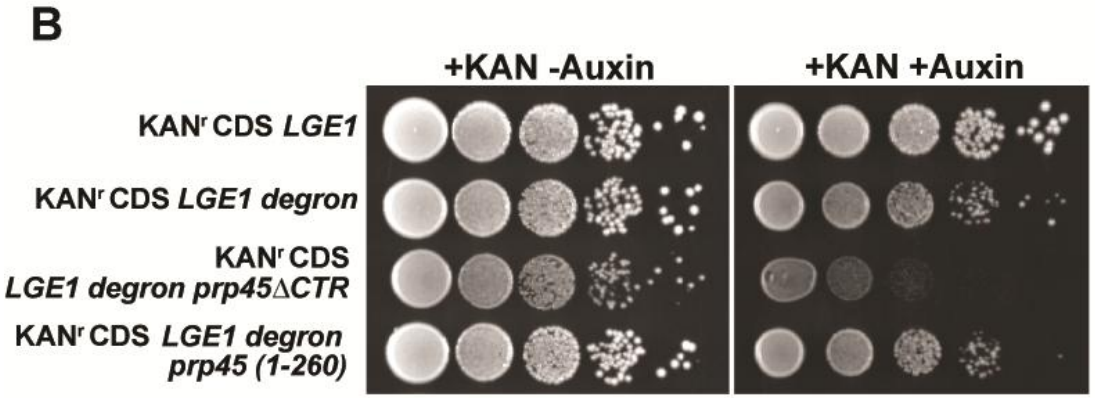

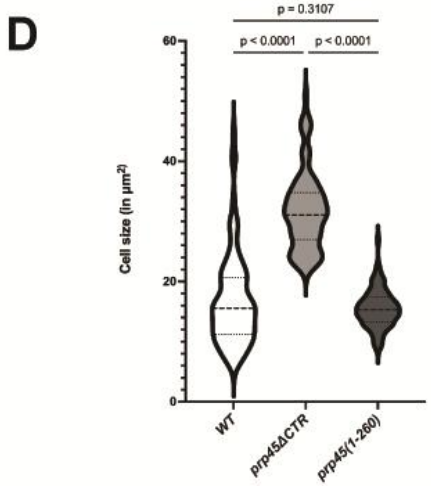
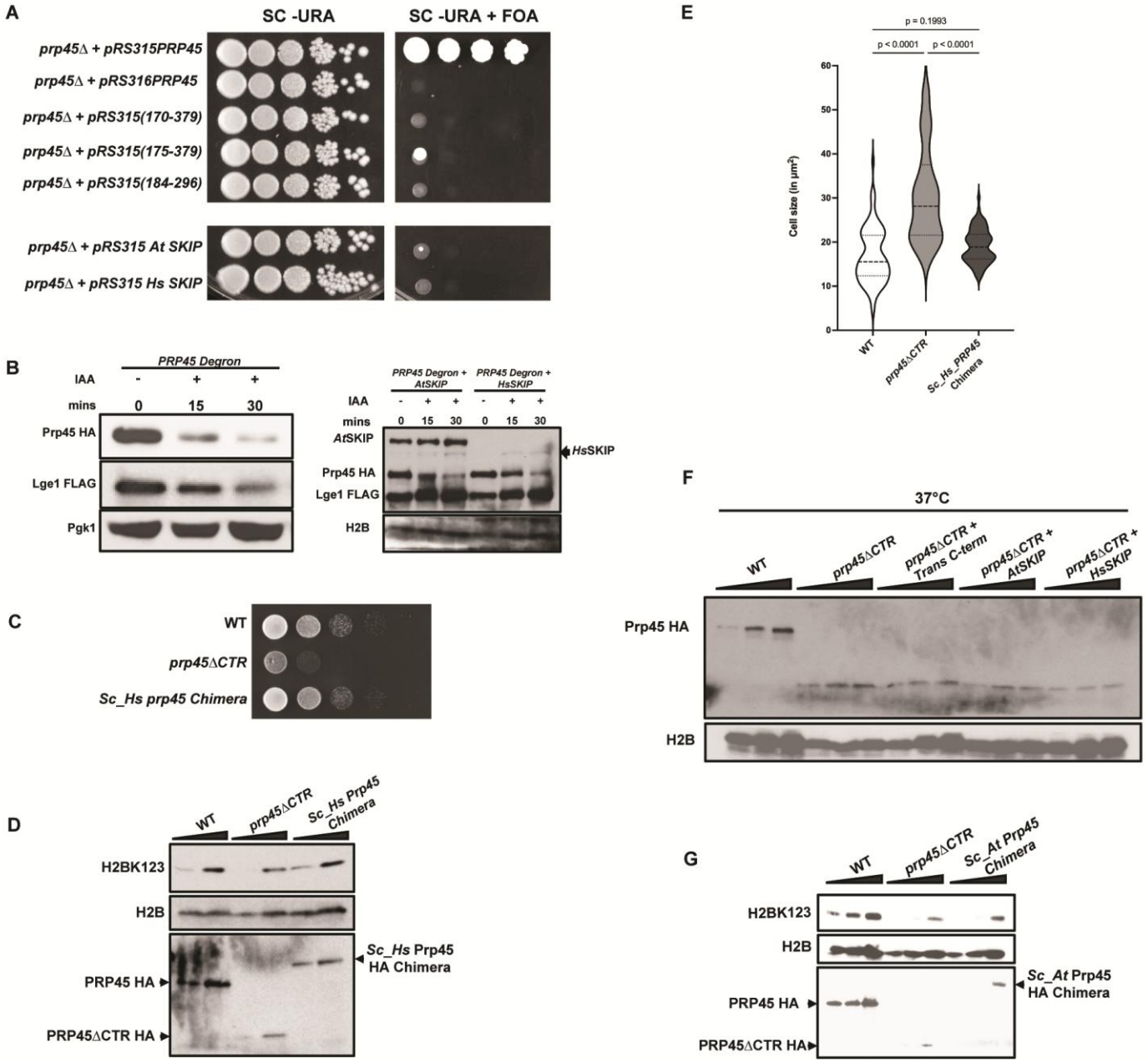
Supplementary figure 6